Fate of long-lived trace species near the Northern Hemispheric tropopause

Zahn, Andreas; Neubert, Rolf; Maiss, Manfred; Platt, Ulrich

Published in:
Journal of geophysical research-Atmospheres

DOI:
10.1029/1998JD100106

Publication date:
1999

JOURNAL OF GEOPHYSICAL RESEARCH, VOL. 104, NO. D11, PAGES 13,923–13,942, JUNE 20, 1999

Fate of long-lived trace species near the Northern Hemispheric tropopause: Carbon dioxide, methane, ozone, and sulfur hexafluoride

Andreas Zahn,[1,2] Rolf Neubert,[3] Manfred Maiss,[4] and Ulrich Platt[1]

Abstract. The mixing ratios of CO_2, CH_4, O_3, and SF_6 were measured in 118 whole air samples collected onboard a Transall C-160 aircraft around the NH extratropical tropopause in the winters 1993-1994 and 1994-1995. The samples originate mainly from the upper troposphere ($\sim$ 7 km) and partly from the lowermost stratosphere up to altitudes of 12 km. With help of 7-day back trajectories the potential temperature θ of an air mass in the free troposphere was established to be a reliable measure of the average latitude the air mass spent the last week before sampling. The potential temperature are thus interpreted in terms of a "representative latitude" allowing -1- for the creation of representative meridional trace gas profiles in the troposphere that show a lower scatter than if the data were plotted versus the sampling latitude itself and -2- for the distinction of different types of air masses. For example, by categorizing the sampled air masses by their potential temperatures and by their trace gas composition, the 300 K θ-surface was identified to separate cold polar air from warmer subtropical air. The 300 K θ-surface is thus found to mark the polar front in the wintertime upper troposphere and can be viewed as the lowest isentrope that allows quasi-isentropic cross-tropopause transport. The midlatitude upper troposphere was frequently affected by surface air resulting in a positive correlation of CH_4, SF_6, and O_3. In contrast, in the arctic upper troposphere and in the lowermost stratosphere, both CH_4 and SF_6 were negatively correlated with O_3. Surprisingly, variable CO_2 levels (spanning $\sim$14 ppm) found just above the ozonopause point to intensive mixing of tropospheric air into the lowermost stratosphere. From the high SF_6 growth rate of nearly 7% per year a clear aging of the observed air masses since their entry into the stratosphere could be inferred. This SF_6 age was rather high, for example around 2 years at an altitude of 11.5 km and thus just 3.5 km above the dynamical tropopause.

1. Introduction

Recent experimental and theoretical studies clearly indicated that the 'classical understanding' of the tropopause as the most crucial regulating system that determines the amount of air entering/leaving the stratosphere cannot be sustained any longer [*Holton et al.*, 1995, and references therein]. For quantifying residence times of trace gases in the stratosphere, the stratosphere rather should be divided in two reservoirs that show different turnover times τ: (1) the "overworld" restricted at the top by the stratopause and at the bottom by the 380-440 K potential temperature surface [*Rosenlof et al.*, 1997] showing a mean τ of 4-5 yr, and (2) the "lowermost stratosphere" lying underneath and extending down to the tropopause [*Hoskins*, 1991] showing a mean τ of 5-8 mon. It is believed that predominantly wave-induced zonal forces acting in the extratropical stratosphere drive the global-scale meridional circulation in which mass is pulled upward and poleward in the tropics and thereafter is pushed downward from the overworld into the extratropical lowermost stratosphere [*Haynes et al.*, 1991].

Nevertheless, the various transport processes coupling lowermost stratosphere and troposphere such as tropopause foldings, cut-off lows and small-scale laminated structures are still of great interest [*Appenzeller et al.*, 1996a; *Beekmann et al.*, 1997; *Langford et al.*,

[1]Institut für Umweltphysik, University of Heidelberg, Heidelberg, Germany.
[2]Now at Max-Planck Institute for Chemistry, Mainz, Germany.
[3]Centrum voor Isotopenonderzoek, University of Groningen, Groningen, Netherlands.
[4]Max-Planck Institute for Chemistry, Mainz, Germany.

Paper number 1998JD100106.
0148-0227/99/1998JD100106$09.00

1996; *Newman and Schoeberl*, 1995]. Recent aircraft campaigns and model calculations confirmed that the fate of many trace species in the lowermost stratosphere and upper troposphere is not sufficiently understood [*Arnold et al.*, 1997; *Borrmann et al.*, 1996; *Bregman et al.*, 1995, 1997; *Fischer et al.*, 1997; *Lelieveld et al.*, 1997; *Solomon et al.*, 1997, *Zahn et al.*, 1998a]. To derive meaningful constraints on the transport cycle and on the chemistry of atmospheric trace constituents, it is useful in experimental studies to record as many species as possible having different sources and sinks. Here we present a comprehensive data set encompassing four trace gases and three isotopomers from 28 flights near the Northern Hemispheric tropopause. In this paper we discuss simultaneous trace gas measurements of carbon dioxide (CO_2), methane (CH_4), ozone (O_3), and sulfur hexafluoride (SF_6); in part 2 we give an overall view about the behavior of the isotopic composition of CO_2 near the tropopause (A. Zahn et al., Fate of long-lived trace species near the Northern Hemispheric tropopause, 2., The isotopic composition of carbon dioxide ($^{13}CO_2$, $^{14}CO_2$, and $C^{18}O^{16}O$), submitted to *Journal of Geophysical Research*, 1999).

The greenhouse gases CO_2 and CH_4 are known to have strong natural and anthropogenic sources and sinks which lead to pronounced geographically dependent seasonal cycles in the troposphere [*Conway et al.*, 1994; *Crutzen*, 1995; *Dlugokencky et al.*, 1994, 1995; *Keeling et al.*, 1996]. Ground-based observations show the highest concentrations in arctic latitudes for both trace gases [*Conway et al.*, 1994; *Denning et al.*, 1995; *Dlugokencky et al.*, 1994]. Maximum CO_2 levels are encountered in the Northern Hemisphere in early spring (~April), but CH_4 peaks in the midwinter months [*Conway et al.*, 1988; *Dlugokencky et al.*, 1995]. Similar seasonal cycles, but which are damped in amplitude and generally delayed by 1-2 months, were found for both trace gases near the Northern Hemispheric tropopause [*Anderson et al.*, 1996; *Bolin and Bischof*, 1970; *Matsueda et al.*, 1993; *Nakazawa et al.*, 1991, 1993, 1997a; *Tanaka et al.*, 1987]. On the other hand, the upper troposphere is also influenced by stratospheric air crossing the tropopause and by long-range transport, which supply this area with air that originates from different CO_2 and CH_4 source and sink regions. In fact, model calculations forecast annual mean CH_4 mixing ratios near the Northern Hemispheric tropopause which are ~(10–80) ppb (10^{-9}mol mol^{-1}) lower than at the ground and which indicate strong longitudinal variations [*Fung et al.*, 1991]. Furthermore, individual air samples collected at a certain latitude near the tropopause have not been representative for the average trace gas composition at that latitude [*Conway and Steele*, 1989; *Marenco et al.*, 1989].

The trace gas O_3 plays an essential role in the short- and long-wave radiative budget of the Earth and is, moreover, involved in the chemistry of almost all major trace gas families [*Brasseur and Solomon*, 1986]. Besides that, for studying stratosphere-to-troposphere exchange, O_3 has frequently been exploited as tracer of stratospheric air because of its large positive gradient across the tropopause [*Danielsen*, 1968; *Langford et al.*, 1996, and references therein]. Experimental and theoretical studies showed that the major O_3 source in the upper troposphere is likely to be the intrusion of stratospheric air and subsequent mixing to lower altitudes [*Gregory et al.*, 1992; *Mauzerall et al.*, 1996]. For instance, during extensive aircraft campaigns in the 6-8 km altitude range of the mid-latitudes and high-latitudes, exactly where our flights took place, roughly 41-57% of the air masses showed signatures of stratospheric intrusions [*Browell et al.*, 1992a, 1994]. Local photochemical O_3 formation and O_3 transported from industrialized areas do not appear to play a major role in the high-latitude free troposphere [*Gregory et al.*, 1992].

The mainly man-made trace gas SF_6 [*Harnish and Eisenhauer*, 1998] is commonly accepted as a powerful transport tracer because of its long atmospheric lifetime of 800-3200 years and its strong global mean increase rate of 6.9% yr^{-1} to date [*Geller et al.*, 1997, *Maiss et al.*, 1996]. Since ~94% of SF_6 is emitted in the Northern Hemisphere [*Maiss et al.*, 1996], a distinct meridional dependent distribution exists that peaks in the mid-latitudes and high-latitudes of the Northern Hemisphere [*Levin and Hesshaimer*, 1996; *Geller et al.*, 1997]. Besides ground-based measurements, only eight vertical balloon-borne SF_6 profiles ranging from 6 to 34 km are available to date [*Harnisch et al.*, 1996; *Patra et al.*, 1997]. They are characterized by a monotonous decrease above the tropopause caused by the growing "age" of the air with increasing altitude.

2. Experiment

From December to March in the years 1991-1992 to 1994-1995 a total of 86 flights (650 flight hours) were performed with a Transall C-160 aircraft. The major interest was to study stratosphere-troposphere exchange by assessing in situ measurements of different long-lived trace gases and of their isotopic composition [*Zahn et al.*, 1998a,b]. Most data presented here were collected in the winters 1993-1994 and 1994-1995 at a pressure level of ~400 hPa corresponding to an altitude of ~7 km. The flights embraced the latitudes from 47° to 86°N and the longitudes from 9°W to 29°E, in which most flights took place in the European Arctic (see Figure 1). In February 1995 the experiment was flown on a Cessna Citation II twin jet aircraft. Three samples were taken at altitudes of 10-12 km or ~200 hPa. Because of technical problems, CO_2, its isotopic composition, and CH_4 could only be measured reliably on one sample.

The ambient O_3 level was measured with a UV absorption monitor (Horiba APOE-350E). A pressure and temperature calibration of the monitor inside a climate chamber suggests an error of $< 3\%$ for O_3 mixing ratios up to 400 ppb.

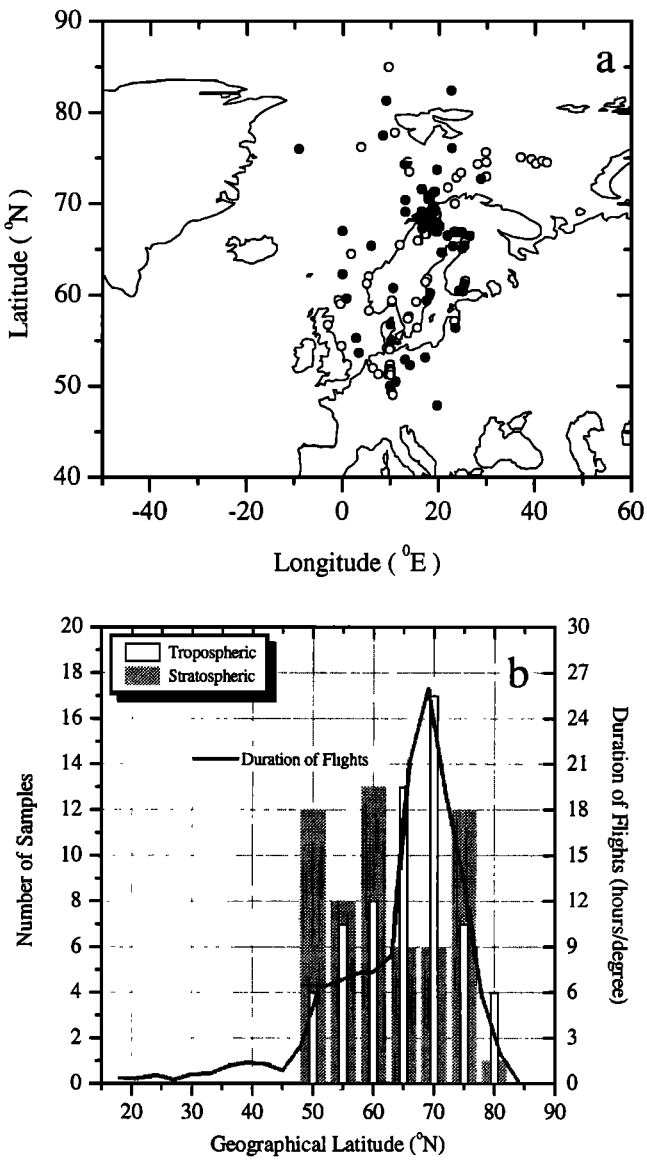

Figure 1. (a) Flight area with sampling locations (dots). (b) Number of samplings separated in 5° meridional bands where light bars indicate tropospheric samples, shadded bars indicate stratospheric samples, and the straight line indicates the average flight time encompassing all 86 flights conducted between December 1991 and April 1995 in hours per degree latitude.

For detecting the trace gases CO_2, CH_4, and SF_6, up to eight glass flasks (1 L) closed with two teflon O-ring stopcocks (Glass Expansion, Australia) were filled with 1.5 L (STP) ambient air by using a teflon sealed compressor. As preflight preparation, the flasks were heated to 300°C while flushing with dry nitrogen. After cooling the flasks were flushed again and filled to a light overpressure with dry background air. During sample collection the incoming air was dried with magnesium perchlorate ($Mg(ClO_4)_2$) (dew point < -60°C). Accordingly, collected water vapor could not condense on the flask wall and exchange of oxygen isotopes between H_2O and CO_2 at the flask wall was efficiently prevented [*Gemery et al.*, 1996].

Various tests were performed in order to quantify possible changes in the sample composition during flask storage. No change in the trace gas mixing ratios nor in the CO_2 isotope composition beyond the range of uncertainties known from flask pair sampling [see *Trolier et al.*, 1996] was found. The trace gases were measured by gas chromatography using a Siemens GC-FID for CO_2 and CH_4 and an electron capture detector (Shimadzu GC-8AIE) for SF_6 described by *Maiss et al.* [1996]. All samples were analyzed 2 or 3 times, resulting in errors of 0.8 ppm for CO_2, 15 ppb for CH_4, and 1.1% for SF_6.

3. Comparison of Thermal, Dynamical, and Ozone Tropopause

For quantifying the vertical distance of the aircraft relative to the tropopause, European Centre for Medium Range Weather Forecast (ECMWF) temperature and potential vorticity analyses were used. The data were provided at 6-hour intervals with a horizontal resolution of 0.5° × 0.5° (T213) at 31 model levels, allowing for the extraction of both the thermal and the dynamical tropopause. Since this observation is discussed in more detail elsewhere (A. Zahn et al., Comparison of thermal, dynamical, and ozone tropopause near Northern Hemisphere tropopause folds, manuscript

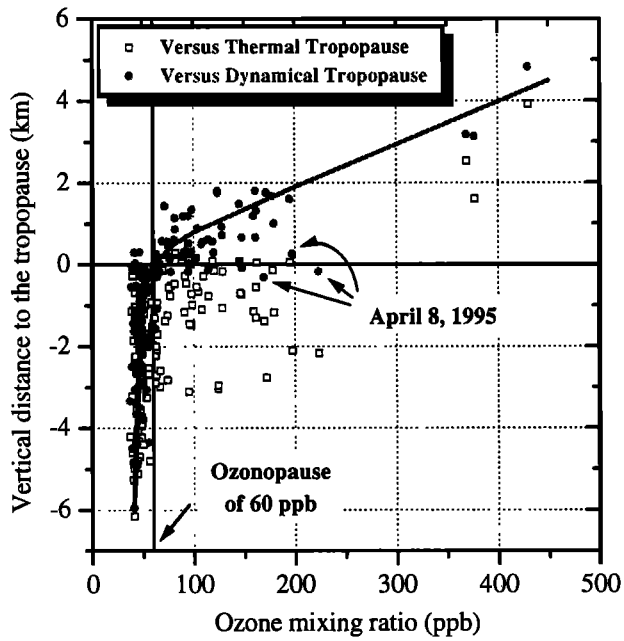

Figure 2. Vertical distance of the aircraft to the thermal tropopause (open squares) and to the altitude of the 2 potential vorticity units (PVU) surface (dots and line displaying the smoothed profile) as function of the O_3 mixing ratio of each sample. A dynamical tropopause of 2 PVU excellently coincides with an ozonopause of 60-80 ppb. One single exception is the last flight of the year (April 8, 1995), which points to temporal variation of the PV value defining the dynamical tropopause.

in preparation, 1999), we only note here that near the polar front the dynamical tropopause rather than the thermal tropopause was generally found to be the appropriate parameter to distinguish between tropospheric and stratospheric air. An example is given in Figure 2, where the vertical distances of the aircraft to the dynamical tropopause, here defined as the height of the 2 Potential Vorticity Unit (PVU) surface (1 PVU = $10^{-6}\,\mathrm{K\,m^2\,kg^{-1}s^{-1}}$), and to the thermal tropopause are plotted as a function of the O_3 mixing ratio at flight level. During our study an O_3 mixing ratio of 60 ppb was found to correspond to the ozonopause (see section 4). Figure 2 clearly indicates that the thermal tropopause typically does not agree with the in situ detected ozonopause. Both quantities can differ by up to 3 km, a feature already observed by *Bethan et al.* [1996], mostly associated with cyclonic conditions. In contrast, the ozonopause height coincides much better with the altitude of the 2 PVU surface; therefore in this study, solely the dynamical tropopause is used.

4. Results and Discussion

All samples were taken in the winter months of December to the beginning of April, north of 48°N. Therefore insignificant photochemical production of O_3 can be assumed within the observation area [*Gregory et al.*, 1992], and O_3 is likely to be a reliable tracer of stratospheric air near the tropopause. During all flights, ambient air with O_3 mixing ratios above 60 ppb were always associated with low levels of H_2O (which additionally showed an unexpected isotopic composition [*Zahn et al.*, 1998a]) and with high PV [*Zahn et al.*, 1998b] and therefore could clearly be assigned to stratospheric origin. The same ozonopause definition (60 ppb) was used by *Conway and Steele* [1989], who conducted simultaneous CO_2, CH_4, and O_3 measurements in the arctic troposphere, as well. Accordingly, samples with O_3 levels above 60 ppb were viewed as "stratospheric," below this boundary as "tropospheric."

4.1. The Tropospheric Data

All together 58 samples could be attributed to tropospheric air (see Table 1). Unfortunately, this small number of samples makes it difficult to identify possible seasonal cycles or any meridional gradient of the measured trace gases. As air parcels of highly different origin and history were sampled, for instance, a simple plot of the data versus latitude shows strong scatter and does not give representative meridional trace gas profiles. As we will show now, the potential temperature of a tropospheric air mass can be a more suitable marker for its meridional origin than the instantaneous latitude itself.

4.1.1. The potential temperature used as tracer for N-S transport. In Figure 3, the ambient potential temperatures θ encountered during each individual sample collection are plotted as a function of the respective sampling latitude φ (dots). Although the aircraft kept a constant pressure level of 397 ± 24 hPa ($1\,\sigma$ variation), these potential temperatures largely scatter between 286 and 314 K and do not follow the expected gradual decrease with latitude. On the other hand, the bold line, which is the mean profile averaging the complete flight time of 650 hours, varies almost linearly with latitude. Apparently, the large variety of different transport phenomena taking place in the free troposphere such as -1- adiabatic movement spreading over large distances and timescales, -2- sporadic short-term diabatic transport caused by convective updrafts originating in the lower troposphere, or -3- long-term diabatic energy dissipation due to radiative cooling (e.g., $1-2\,\mathrm{K\,day^{-1}}$ around the tropopause in the polar night), which all together are responsible for the vigorous scatter found for individual sample spots, are averaged out in data of only 650 hours in the huge flight area that ranged from 17° to 86°N.

Before presenting back trajectory calculations affirming this close relation between potential temperature θ and latitude φ and before giving an explanation for it we first derive an analytical relation between both quantities. Note that the area of latitudinal bands diminishes with the cosinus of the latitude. Thus the likelihood of sampling air originating from the south rather than from the north increases with sampling latitude. As a consequence, the observed θ-φ relation (bold line in Figure 3) has the tendency to assign potential temperatures at high latitudes that are slightly too high, so that simply a linear θ-φ relation over the whole area examined is assumed (dashed line). We call this quantity the representative latitude

$$\phi \;=\; 90°\mathrm{N} \;-\; 1.73\,°/\mathrm{K}\,(\theta - 285\,\mathrm{K}) \qquad (1)$$

with θ in Kelvin. As expected, the mean latitude of sampling ($\overline{\varphi} = 65.5°$N) approximately corresponds to $\overline{\phi} = 66.8°$N when using the mean potential temperature during sampling of $\overline{\theta} = 298.4$ K.

One can argue that changes in the flight altitude lead to corresponding variations in the potential temperature. However, all samples were gathered at a constant pressure of 397 ± 24 hPa ($1\,\sigma$ variation). On the basis of the typical temperature lapse rate of 6-7 $\mathrm{K\,km^{-1}}$ there [*Thuburn and Craig*, 1997], pressure variations of ± 24 hPa only correspond to changes of $\theta \approx 1.3$ K and, applying (1), in the representative latitude, of $\leq 2.3°$. Higher deviations in ϕ would only be expected within baroclinic zones which, however, have always been accompanied with stratospheric intrusions. Even these cases are excluded in the present section because only tropospheric samples are addressed here.

Figure 3 shows that in the mean over hundreds of flight hours the potential temperature of a tropospheric air mass is a close function of its instantaneous latitude. However, in order to exploit the potential temperature

Table 1. Tropospheric Samples Characterized by O_3 Mixing Ratios Below 60 ppb

	Date	Time, GMT	φ, °N	ϑ, °E	T, °C	H, km	P, hPa	θ, K	TP, km	O_3, ppb	CO_2, ppm	CH_4, ppm	SF_6, ppt
1	Jan. 25, 1994	08:16	71.3	19.3	−52.5	6.63	391	289.8	7.76	42.1	361.9	1.833	...
2	Jan. 25, 1994	08:54	73.7	19.7	−53.0	6.61	391	289.0	7.55	47.0	363.3	1.813	...
3	Jan. 25, 1994	13:38	69.1	13.2	−55.9	6.90	376	288.5	7.42	42.0	365.8	1.832	...
4	Jan. 28, 1994	09:22	70.4	13.1	−52.4	6.42	410	285.9	7.86	40.5	366.6	1.851	...
5	Jan. 28, 1994	10:57	65.4	5.9	−43.7	6.45	410	297.2	8.90	47.8	364.8	1.842	...
6	Jan. 28, 1994	12:24	59.6	1.0	−49.8	7.12	375	296.7	7.21	49.3	366.8	1.838	...
7	Feb. 8, 1994	13:49	59.4	16.5	−42.1	7.09	392	303.2	9.03	52.2	361.1	1.808	...
8	Feb. 15, 1994	14:11	81.3	9.1	−49.1	6.49	392	294.0	6.80	51.0	362.2	1.819	...
9	Feb. 15, 1994	17:04	69.2	18.4	−39.9	7.75	359	313.8	11.45	48.3	360.3	1.795	...
10	Feb. 16, 1994	10:54	64.7	20.6	−34.8	6.59	427	305.2	10.25	42.8	366.5	1.806	...
11	Feb. 16, 1994	12:09	60.2	18.3	−32.6	6.68	427	307.9	11.56	40.3	369.2	1.801	...
12	Feb. 16, 1994	14:01	55.0	10.2	−33.6	6.67	427	306.7	10.47	47.6	367.7	1.815	...
13	Feb. 16, 1994	15:16	50.0	10.0	−33.1	6.30	447	303.4	8.19	45.2	365.1	1.815	...
14	Mar. 11, 1994	11:45	47.9	19.8	−25.4	6.55	445	313.6	10.90	56.0	376.1	1.828	...
15	Mar. 11, 1994	15:27	61.2	25.4	−39.3	7.74	375	310.7	10.80	53.3	373.0	1.799	...
16	Mar. 13, 1994	16:06	76.1	22.8	−45.2	6.37	410	295.2	9.27	48.6	361.6	1.803	...
17	Mar. 13, 1994	18:03	76.0	−9.0	−48.9	6.34	410	290.5	8.40	47.2	362.2	1.831	...
18	Mar. 13, 1994	19:34	74.3	13.0	−51.1	6.92	375	295.0	9.11	49.6	363.6	1.860	...
19	Mar. 13, 1994	20:53	69.2	19.3	−51.9	6.96	376	293.9	7.87	48.7	363.6	1.850	...
20	Dec. 13, 1994	09:43	52.9	13.1	−24.4	6.14	465	310.8	10.97	39.7	362.2	1.793	...
21	Dec. 13, 1994	13:53	66.9	19.7	−52.2	7.40	343	301.1	7.48	39.6	370.2	1.848	...
22	Dec. 15, 1994	09:51	68.6	18.3	−20.1	3.45	642	288.3	9.40	40.8	359.2	1.833	...
23	Dec. 15, 1994	10:38	68.5	18.3	−36.8	6.46	426	302.6	9.52	41.4	361.5	1.812	...
24	Dec. 15, 1994	11:13	66.9	23.3	−40.1	6.40	427	298.4	6.10	46.9	362.7	1.805	...
25	Dec. 17, 1994	13:48	71.6	16.5	−46.9	6.93	391	297.0	7.04	44.4	361.1	1.810	...
26	Dec. 17, 1994	15:22	77.5	8.4	−50.2	6.82	391	292.7	6.53	41.5	364.9	1.832	...
27	Dec. 17, 1994	16:30	82.4	22.7	−48.6	6.80	391	294.8	9.47	42.8	366.2	1.838	...
28	Dec. 17, 1994	18:44	74.6	13.6	−45.6	6.88	391	298.8	9.36	44.1	363.3	1.784	...
29	Dec. 20, 1994	12:22	67.0	0.0	−52.2	7.09	375	293.5	7.64	38.7	364.4	1.843	...
30	Dec. 20, 1994	13:24	62.3	0.0	−50.2	7.14	375	296.2	7.64	52.2	364.5	1.826	...
31	Dec. 20, 1994	15:01	55.3	2.9	−46.1	7.25	376	301.5	7.96	46.9	364.5	1.799	...
32	Dec. 20, 1994	15:23	53.6	3.5	−48.7	7.92	342	306.0	8.18	46.6	364.1	1.804	...
33	Jan. 11, 1995	10:29	56.8	10.0	−43.4	6.28	427	294.2	7.92	41.0	370.2	1.836	3.504
34	Jan. 11, 1995	11:27	60.8	10.6	−43.4	6.24	427	294.2	8.25	54.9	367.1	1.811	3.456
35	Jan. 12, 1995	09:36	68.4	16.0	−46.1	6.30	427	290.6	7.45	46.0	362.6	1.833	3.549
36	Jan. 12, 1995	11:03	70.8	17.8	−51.5	6.80	393	290.5	8.05	45.6	362.7	1.831	3.584
37	Jan. 12, 1995	11:53	67.3	16.7	−48.8	6.84	393	294.1	7.40	48.6	360.7	1.831	3.469
38	Jan. 12, 1995	13:18	67.6	20.0	−49.6	6.88	393	293.0	7.98	48.7	360.6	1.820	3.530
39	Jan. 15, 1995	08:19	65.1	24.9	−42.1	6.25	426	296.0	7.60	42.7	360.8	1.826	3.509
40	Jan. 15, 1995	08:50	66.5	21.9	−49.6	6.25	426	286.4	6.22	42.1	362.8	1.852	3.547
41	Jan. 15, 1995	09:44	69.1	16.5	−54.0	6.63	392	287.5	6.95	49.7	362.1	1.828	3.520
42	Jan. 15, 1995	11:17	67.5	18.5	−51.1	6.67	393	291.1	6.80	51.6	362.6	1.845	3.485
43	Jan. 15, 1995	12:53	65.4	23.1	−49.6	6.78	393	293.1	7.35	58.6	363.1	1.815	3.474
44	Jan. 15, 1995	14:38	67.5	20.2	−51.5	6.75	393	290.6	6.80	46.7	364.3	1.839	3.481
45	Jan. 17, 1995	12:59	60.6	25.0	−34.9	7.32	391	312.6	12.20	44.4	378.6	1.805	3.457
46	Jan. 17, 1995	14:07	56.4	23.5	−34.5	7.40	391	313.2	12.30	44.3	371.5	1.781	3.478
47	Jan. 17, 1995	15:28	53.2	17.3	−34.1	7.40	391	313.7	11.90	38.8	369.0	1.801	3.439
48	Jan. 17, 1995	16:01	52.3	14.1	−35.3	7.40	391	312.2	10.78	42.2	368.4	1.823	3.430
49	Jan. 17, 1995	16:46	50.5	11.2	−35.7	7.37	391	311.6	10.70	36.6	369.5	1.799	3.414
50	Jan. 30, 1995	14:53	68.0	16.7	−54.6	6.72	392	286.7	7.60	46.9	366.1	1.799	3.475
51	Jan. 30, 1995	15:08	67.8	19.7	−55.1	6.72	392	286.1	7.39	54.7	364.6	1.822	3.484
52	Jan. 31, 1995	07:03	65.4	25.4	−47.0	6.56	409	293.0	9.06	38.5	366.8	1.871	3.585
53	Jan. 31, 1995	10:34	60.5	24.3	−45.1	6.63	410	295.4	8.40	55.4	362.8	1.809	3.471
54	Mar. 22, 1995	17:25	66.5	26.5	−38.1	6.98	392	308.3	10.77	49.9	368.4	1.832	...
55	Mar. 22, 1995	17:40	66.9	24.8	−35.6	6.88	392	311.6	11.28	43.8	371.0	1.830	3.583
56	Mar. 26, 1995	16:40	72.7	28.9	−51.8	6.87	374	294.3	8.35	59.1	367.4	1.826	...
57	Mar. 26, 1995	18:41	70.5	18.0	−53.4	6.85	374	292.2	7.02	59.5	369.7	1.834	3.669
58	Mar. 26, 1995	19:39	70.7	18.0	−54.8	6.86	374	290.3	7.15	58.2	368.6	1.816	...
	Jan. 6		65.5	16.1	−44.9	6.81	398	298.3	8.67	46.7	365.8	1.822	3.483

The abbreviations are defined as follows: φ and ϑ, latitude and longitude of sampling; T, temperature; H, altitude; P, pressure; θ, potential temperature; and TP, height of the dynamical tropopause. Last row: Mean of all samples (except sample 22), whereas the CO_2 and SF_6 data were adjusted to January 1, 1995 values (see section 4.1.2).

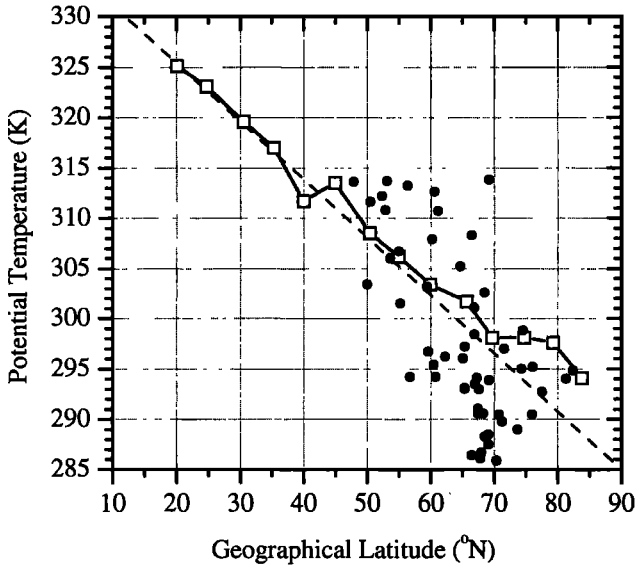

Figure 3. Potential temperature at flight altitude as a function of latitude. Dots indicate the tropospheric samples listed in Table 1. Open squares connected with a straight line indicate the mean profile considering the parts of all 86 flights that took place in the troposphere. The dashed line indicates the proposed analytical relation, called the representative latitude (see (1)).

as a tracer which attributes an individual air mass to the latitude where the air mass spent most of the time we need to prove the correctness of the θ-φ relation for individual air parcels. Therefore isentropic 7-day back trajectories were calculated for those samples which were characterized by the highest deviations in their trace gas composition from the mean at the respective representative latitude (these samples are designated in Figure 6 by their sample numbers). The result is shown in Figure 4, where three different latitude definitions are compared: -1- the latitude of sampling φ, -2- the "trajectory latitude" φ' defined as the mean latitude of the trajectory the last 6 days before sampling, and -3- the representative latitude ϕ as defined in (1). Figures 4a and 4c simply reflect that the meridional origin of a tropospheric air parcel is described poorly by its latitude of observation but rather realistically by its representative latitude. Remembering that the largest "bite outs" and thus the fewest suitable air parcels were considered, this finding supports the representative latitude ϕ as an excellent measure for the mean latitude a tropospheric air parcel spent the last week before sampling.

As the explanation for the θ-φ relation is equivalent, we first present a further observation, namely, that the local tropopause height holds similar information to the representative latitude (see Figure 5). As in mid-latitudes and high-latitudes, the local tropopause height varies strongly in time and space; only a weak correlation to the instantaneous sampling latitude is visible in Figure 5a ($R = -0.56$). The correlation is much closer ($R = -0.89$) when comparing with the mean latitude over the last 6 days, here represented by the trajectory

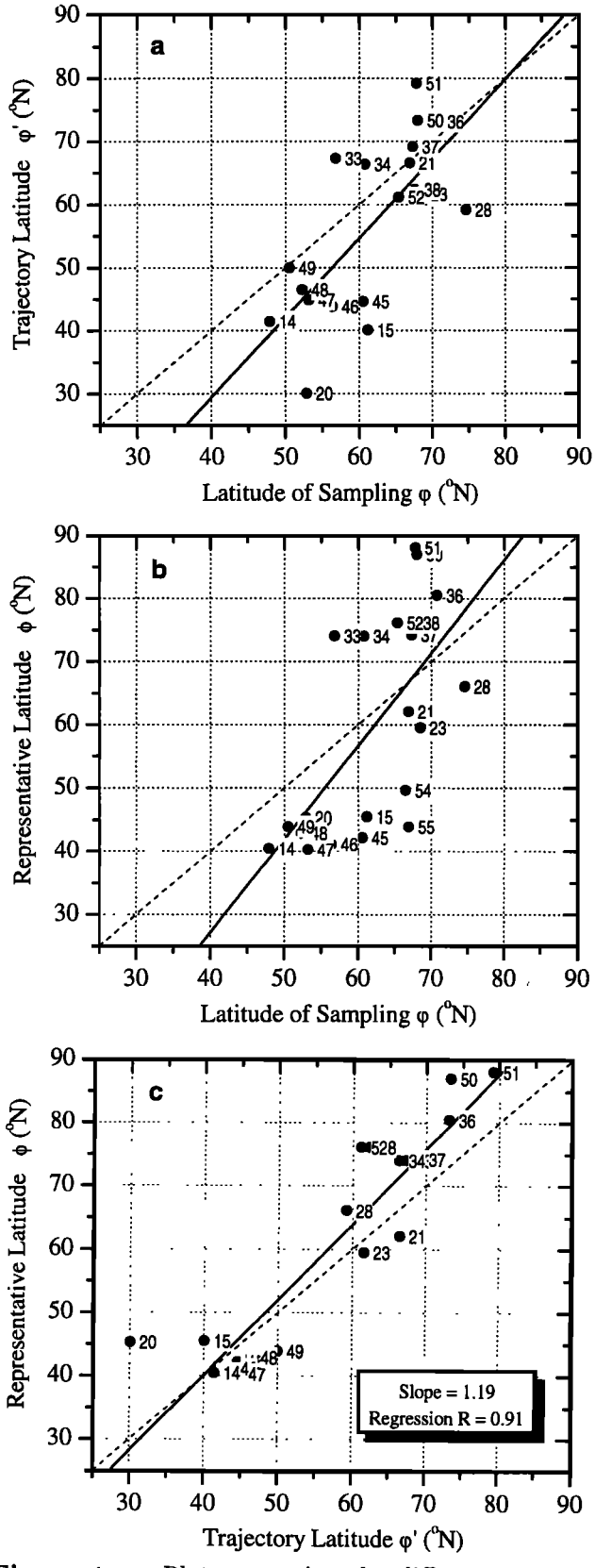

Figure 4. Plot comparing the different types of latitude definitions used: **(a)** $\varphi' = -21°N + 1.26\varphi$ ($R = 0.71$); **(b)** $\phi = -32°N + 1.47\varphi$ ($R = 0.64$), and **(c)** $\phi = -7°N + 1.19\varphi'$ ($R = 0.91$). Considered are only those samples (labeled with the numbers given in Table 1) for which trajectory calculations are available. Dashed lines mark the respective 1:1 relations. Solid lines are regression lines.

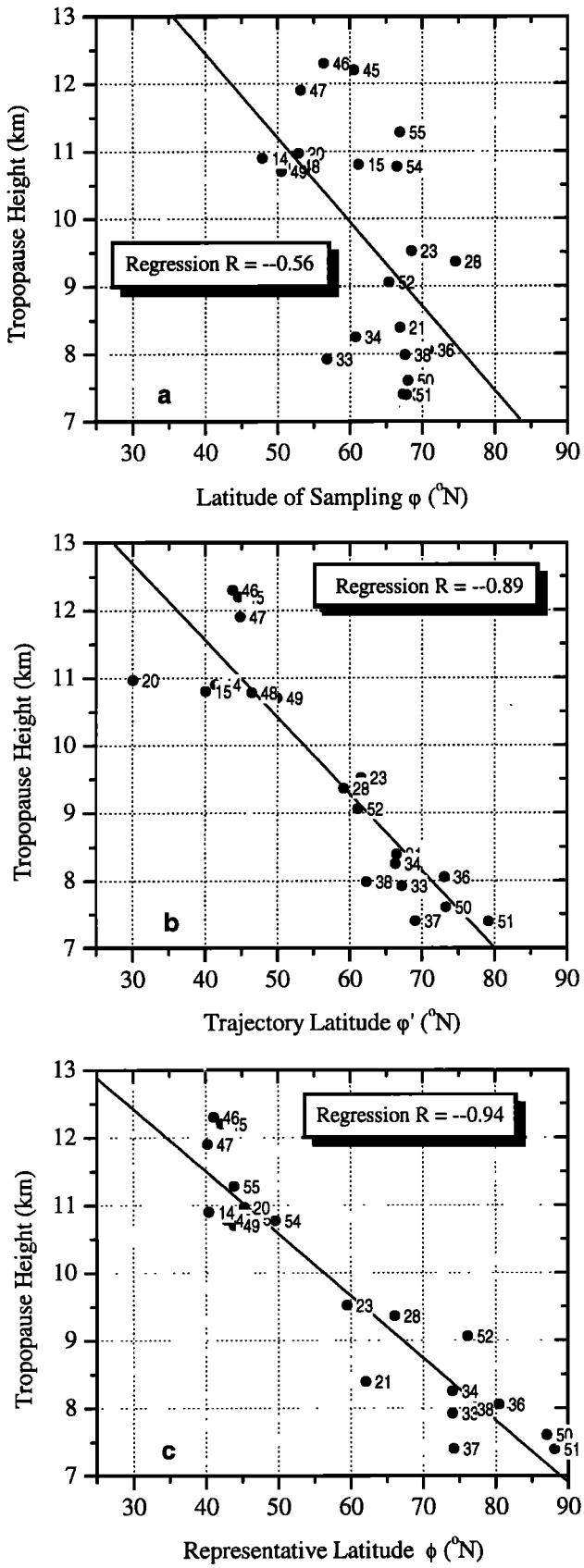

Figure 5. Dynamical tropopause height (TP) as a function of the different types of latitude definitions used: **(a)** TP = 17.4 km − 0.125φ (R = −0.56), **(b)** TP = 16.1 km − 0.114φ' (R = −0.89), and **(c)** TP = 15.2 km − 0.092φ' (R = −0.94). Considered are only those samples (labeled with the numbers given in Table 1) for which trajectory calculations are available. Solid lines are regression lines.

latitude (Figure 5b), but the correlation to the representative latitude is even better (R = −0.94; Figure 5c).

In the following we will give an explanation for the latter observations, i.e., for the close relation between the meridional origin of a tropospheric air mass, its temperature, and the local tropopause height. First, the altitude of the tropopause is mainly regulated by the thermal structure of the troposphere [*Held*, 1982; *Thuburn and Craig*, 1997]. Thus high temperatures in the lower troposphere, as encountered in the (sub)tropics, always lead to high tropopauses. Second, cyclones/anticyclones generated by the instability of the subpolar jet stream show dynamically induced low/high tropopauses and contain cold/warm air from north/south of the polar front. Both effects link tropospheric temperatures and thus the representative latitude with the instantaneous tropopause height. This coupling persists during adiabatic equatorward/northward excursions of the polar front.

In summary, the meridional origin of a tropospheric air parcel is mirrored in its temperature (here used to define the representative latitude) and in the local tropopause height (Figures 4 and 5). Hence, and as demonstrated in the next section, plotting tropospheric trace gas data versus one of both quantities leads to representative meridional trace gas profiles that show distinctively reduced scatter.

4.1.2. Latitudinal profiles of CO_2, CH_4, O_3, and SF_6. In the following, we try to resolve possible meridional gradients of the analyzed trace gases to learn about the transport pathways from their (mainly ground-based) emission to the mid-latitude and high-latitude troposphere. As the flight area and the synoptic condition in both winters 1993-1994 and 1994-1995 examined here were almost identical, all the data are discussed together. First, possible growth of the trace gases has to be eliminated in order to separate it, inter alia, from eventually existing meridional gradients. Since our limited data set does not permit the inference of possible growth rates of the measured trace gases, we apply numbers given in the literature and adjust the SF_6 and CO_2 data to January 1, 1995 values. For SF_6 we assume a constant secular increase of 6.9% yr^{-1} [*Geller et al.*, 1997; *Maiss et al.*, 1996], for CO_2 we apply the long-term trend of 1.4 ppm yr^{-1} given by *Trolier et al.* [1996].

In Figure 6, the mixing ratios of CO_2, CH_4, O_3, and SF_6 from all tropospheric samples are plotted as a function of the ambient potential temperature during sampling (lower x axis) and of the representative latitude ϕ (upper x axis, see (1)). The scatter in all data sets is considerable. However, when looking in more detail, the profiles exhibit a discontinuity in slope at $\phi \approx$ 60-70°N (it is determined more precisely to be $\phi \approx$ 64°N with the aid of trace gas correlations found south and north of the 300 K isentrope; see section 4.1.4). All trace gases indicate similar meridional profiles north of these latitudes, but south of them, CO_2 decreases with latitude whereas CH_4, O_3, and SF_6 show the opposite behavior. This observation is more clearly visible for mean

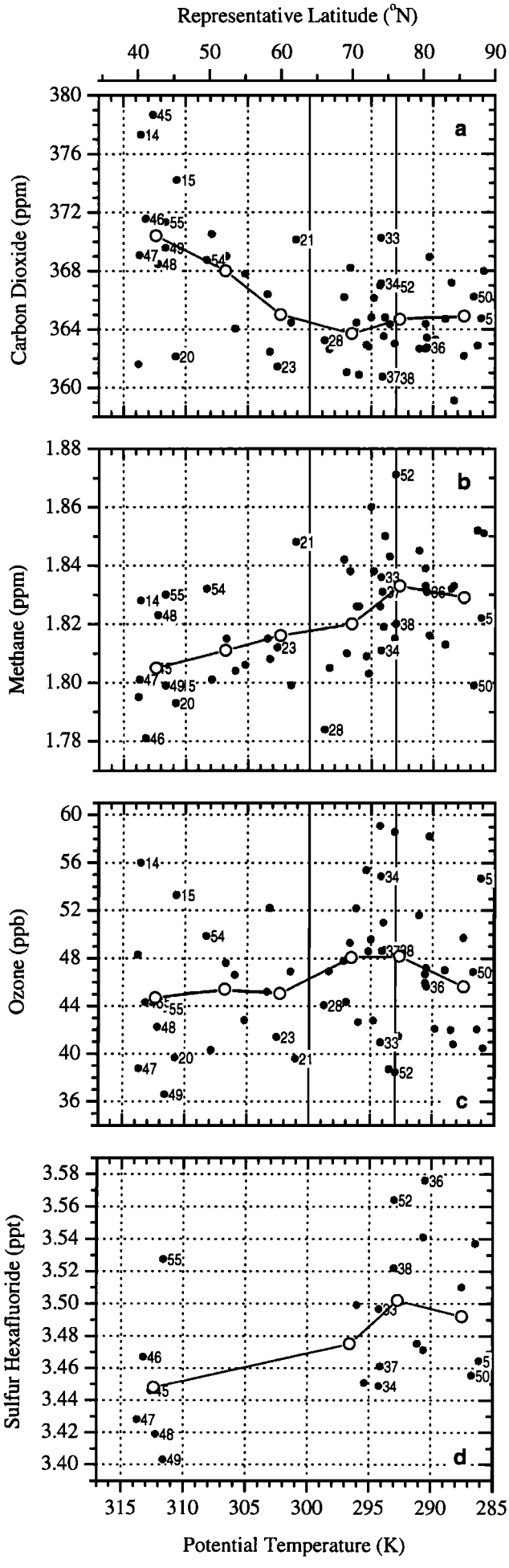

values over 5 K potential temperature intervals (large circles; see also Table 2), which additionally indicate weak scatter over the observation area.

The most likely explanation is that this discontinuity marks the mean latitude of the polar front during our study. Unfortunately, a clear distinction, whether an individual sample was collected north or south of the polar front, in most cases was neither possible with the help of weather charts nor with back trajectory calculations because -1- the aircraft was frequently close to the rapidly varying polar front zone and -2- diabatic processes near the subpolar jet stream restrict the quality of isentropic trajectory calculations. Nevertheless, a rough estimation reveals that about the same number of tropospheric samples was gathered north and south of the polar front; the mean sampling latitude of 65.5°N actually agrees with $\phi \approx 64°$N, where the discontinuity was found. In addition, when plotting all O_3 data (650 hours) as a function of the potential temperature, a sharp maximum at $\theta = 302$ K is visible. This O_3 maximum is due to the intrusion of O_3-rich stratospheric air taking place always at the southern anticyclonic side of the polar front [*Danielsen and Mohnen*, 1977; *Browell et al.*, 1987; *Holton et al.*, 1995, and references therein]. In addition, in various early and fundamental investigations, for example, by *Bergren* [1952], *Reed* [1955], *Staley* [1960], and *Danielsen* [1968], but also more recently [*Danielsen and Mohnen*, 1977; *Hoskins et al.*, 1985], the 300 K isentrope was mostly found to be below the 600 hPa pressure level on the southern side of tropopause folds associated with the polar front, ascended by 3-4 km within the folds and nearly coincided with the dynamical tropopause on its cyclonic side at ~350 hPa (see Figure 12). Hence the potential temperature of an individual air parcel can tentatively be used to distinguish "polar air" ($\theta < 300$ K) and "subtropical air" ($\theta > 300$ K) (this border is only valid around the 400 hPa level). Note that the names for these air masses are of historical origin, i.e., "subtropical air" stands for air south of the polar front, although the polar front can reach the Arctic.

At first glance a plot of our data versus the representative latitude seems to describe the trace gas composition in the upper troposphere quite realistically. However, that kind of display implicates one problem not mentioned yet. As indicated by back trajectory calculations, on average the air masses with the highest potential temperatures (> 310 K) first were encountered at

Figure 6. Tropospheric profiles of **(a)** CO_2, **(b)** CH_4, **(c)** O_3, and **(d)** SF_6 versus the potential temperature at flight level or the representative latitude (see (1)). Samples for which back trajectories are available are labeled with the sample numbers listed in Table 1. Open circles on a straight line indicate mean values binned by potential temperature intervals of 5 K. The vertical straight lines at $\theta = 293$ K and $\theta = 300$ K mark the estimated mean potential temperatures encountered near the arctic front and near the polar front in the upper troposphere (see text).

Table 2. Mean Values of the Tropospheric Data Binned by Potential Temperature Intervals of 5 K

θ K	N	ϕ °N	φ,[a] °N	T,[a] °C	P,[a] hPa	H,[a] km	TP,[a] km	O_3,[b] ppb	CO_2,[b] ppm	CH_4,[b] ppm	SF_6,[b] ppt	CO_2/CH_4,[b] ppm/ppm	CO_2/SF_6,[b] ppm/ppt
285-290	8	85.7	69.5	−53.4	396	6.61	7.3	45.6	364.9	1.829	3.492	199.5	104.3
290-295	18	76.6	69.7	−49.4	396	6.85	7.4	48.2	364.7	1.833	3.502	199.0	104.0
295-300	10	69.9	67.6	−46.0	399	6.71	8.1	48.1	363.7	1.820	3.475	199.8	104.2
300-305	5	59.9	60.0	−42.1	397	6.90	8.5	45.1	365.0	1.816	...	200.9	...
305-310	5	52.2	60.0	−37.6	403	6.97	10.2	45.4	368.0	1.812	...	203.2	...
310-315	10	42.5	57.1	−33.9	399	7.20	11.3	44.7	370.4	1.805	3.448	205.2	107.7

Sample 22 originates from low altitudes and is not included. Abbreviations are defined as θ, potential temperature, and N, number of samples.

[a] Means during sample collection for the representative latitude ϕ (see (1)) and the sampling latitude φ. T, P, H, and TP are as listed in Table 1.

[b] Mean values of the measured trace gases and of the ratios CO_2/CH_4 and CO_2/SF_6. CO_2 and SF_6 data are adjusted to January 1, 1995 values (see section 4.1.2).

$\varphi \approx 57°$N and thus 15° north of the assigned representative latitude of ~42°N, second originated from North America (9 of 11 trajectories) and third, were lifted up by ~100 hPa during the last 5 days before sampling. This northeast and upward directed transport was generally forced by a special type of synoptic condition, that is, a deep trough of the polar front over the Atlantic and an anticyclone above central Europe. This indicates that these air parcels indeed originated from ~35-45°N, but do not necessarily show the trace gas composition typically encountered at that latitude.

Evidence for this suspicion gives the atypical meridional CO_2 profile. South of $\phi = 45°$N, CO_2 ranged between 361 and 379 ppm, in which the latter value can only be found in polluted air masses. Moreover, CO_2 decreased ~6 ppm from 45° to 65°N, on average, whereas previous observations suggest a slight increase of 0-2 ppm at the same latitude range, altitude, and season [*Anderson et al.*, 1996; *Nakazawa et al.*, 1991, 1997a]. On the other side this atypical meridional CO_2 profile cannot only be due to plotting the data versus the representative latitude, because displaying the CO_2 data versus the sampling latitude reveals the same meridional trend (not shown here). Perhaps, most of the samples collected at $\phi = 40 - 50°$N are not typical for these latitudes, but because CO_2 levels beyond 370 ppm were never found further north, this finding hints that the midlatitude troposphere is more frequently affected by surface air than the polar troposphere. This assumption is supported first by *Jacob et al.* [1987], who pointed out that the northwestern Atlantic is often influenced by polluted air from the United States and Europe and second by *Arnold et al.* [1997], who found strong CO_2-, SO_2-, and acetone- (CH_3COCH_3) polluted air in the upper troposphere at 56°N. North of the polar front, no such anthropogenically influenced surface air was discovered in the upper troposphere yet.

Besides this unexpected meridional CO_2 distribution, the CH_4, O_3, and SF_6 profiles (see Figure 6) roughly agree with previous studies, but a few additional features are worth mentioning:

1. Anthropogenically influenced midlatitude air identified by elevated CO_2 levels beyond 368 ppm showed depleted O_3 mixing ratios of 41 ± 3 ppb in January (samples 21, 33, and 45-49), but elevated ones of 55 ± 2 ppb in March (samples 14 and 15), each compared to the typical and quite constant 45-50 ppb. This finding points to the higher O_3 formation potential of polluted,

Table 3. Linear Correlation Coefficients R Between CO_2, CH_4, O_3, and SF_6 Inferred From the Tropospheric Data and the Stratospheric Data

	Troposphere			Stratosphere
	Arctic Air $\theta = 286-293$ K	Polar Air $\theta = 293-300$ K	Subtropical Air $\theta = 300-314$ K	
Number of Samples	18 (10)	19 (6)	20 (6)	60 (39)
O_3 versus SF_6	−0.66 (0.04)	−0.87 (0.03)	0.66 (0.15)	−0.94 (0.00)
CH_4 versus SF_6	0.52 (0.12)	0.75 (0.09)	0.34 (0.50)	0.87 (0.00)
O_3 versus CH_4	−0.51 (0.02)	−0.43 (0.50)	0.12 (0.63)	−0.87 (0.00)
CO_2 versus SF_6	−0.21 (0.56)	0.16 (0.67)	0.23 (0.66)	$< \pm 0.1$
CO_2 versus CH_4	$< \pm 0.1$	$< \pm 0.1$	0.13 (0.36)	0.17 (0.36)
CO_2 versus O_3	$< \pm 0.1$	$< \pm 0.1$	0.18 (0.47)	$< \pm 0.1$

The number of the SF_6 samples (line 4) and the p values, the probability that the linear correlation coefficient R is zero, are given in parentheses.

i.e., NO_x-rich air, in spring based on the stronger exposure to solar radiation compared to January [*Parrish et al.*, 1998].

2. CH_4 and SF_6 show similar latitudinal profiles, both peaking in the Arctic. Aircraft measurements by *Schmidt et al.* [1984] in May 1981 indicated the same CH_4 gradient of ~30 ppb between 40° and 80°N. In contrast, the CH_4 gradient found by *Marenco et al.* [1989] in June 1984 was twice as high, but no meridional change was detected by *Heidt et al.* [1980] in April/May 1978. The meridional SF_6 profiles measured on the ground by *Maiss et al.* [1996] and modeled by *Levin and Hesshaimer* [1996] suggest the highest levels in the midlatitudes. We guess that this difference between the ground-based profile and the upper tropospheric profile is not due to an artifact of our low sample statistic because SF_6 always correlated with CH_4 (see section 4.1.4 and Table 3) for which more samples are available (and which also peaks in the Arctic). Thus we assume that quasi-horizontal transport from the midlatitudes surpasses direct vertical transport from the arctic ground (we believe that the ground-based meridional profile by *Geller et al.* [1997], which peaks in the Arctic, is not representative because only selected, i.e., unpolluted, air masses were taken into consideration).

3. The five samples collected on January 17, 1995 (samples 45-49), indicate surprisingly low SF_6 levels, although high CO_2 mixing ratios ~371 ppm) and back trajectories all originating from the United States point to near-surface air from industrialized zones, which mostly show elevated SF_6 levels.

4. Ozone decreases north of $\phi \approx 75°$N. Since at the same time the distance of the aircraft to the tropopause diminished to only 700 m at $\phi \approx 85°$N (see Table 2), we conclude that the vertical stratosphere-to-troposphere flux has been very limited there.

5. Besides the discontinuity at the polar front, a further structure in the meridional trace gas profiles is visible, namely, all trace gases decrease north of $\phi \approx 75°$N. In addition, the trace gases correlate differently north and south of this latitude (see section 4.1.4). Together, both findings allow us to distinguish arctic air north of $\phi = 75°$N ($\theta < 293$ K) and polar air between $\phi = 64°$ and 75°N ($293\,K < \theta < 300$ K). Note, in contrast to polar air, arctic air originates always from very high latitudes and is colder than polar air by definition.

4.1.3. Seasonality of CO_2, CH_4, and O_3. The observed seasonal behavior of CO_2, CH_4, and O_3 agrees with previous studies (see Figure 7). From December to March, CO_2 increases $\sim 1.4 \pm 0.5$ ppm mon^{-1}, O_3 increases $\sim 2.4 \pm 0.6$ ppb mon^{-1}, but CH_4 changes insignificantly, 1.8 ± 2.5 ppb mon^{-1}.

Similar weak seasonal CO_2 changes were found during winter on the ground [*Conway et al.*, 1994] and in the free troposphere [*Nakazawa et al.*, 1997a] (but the phase delay and the different amplitude of the CO_2 seasonality between ground and upper troposphere detected by *Anderson et al.* [1996] cannot be studied here). The observed O_3 increase is only 50% of that found by

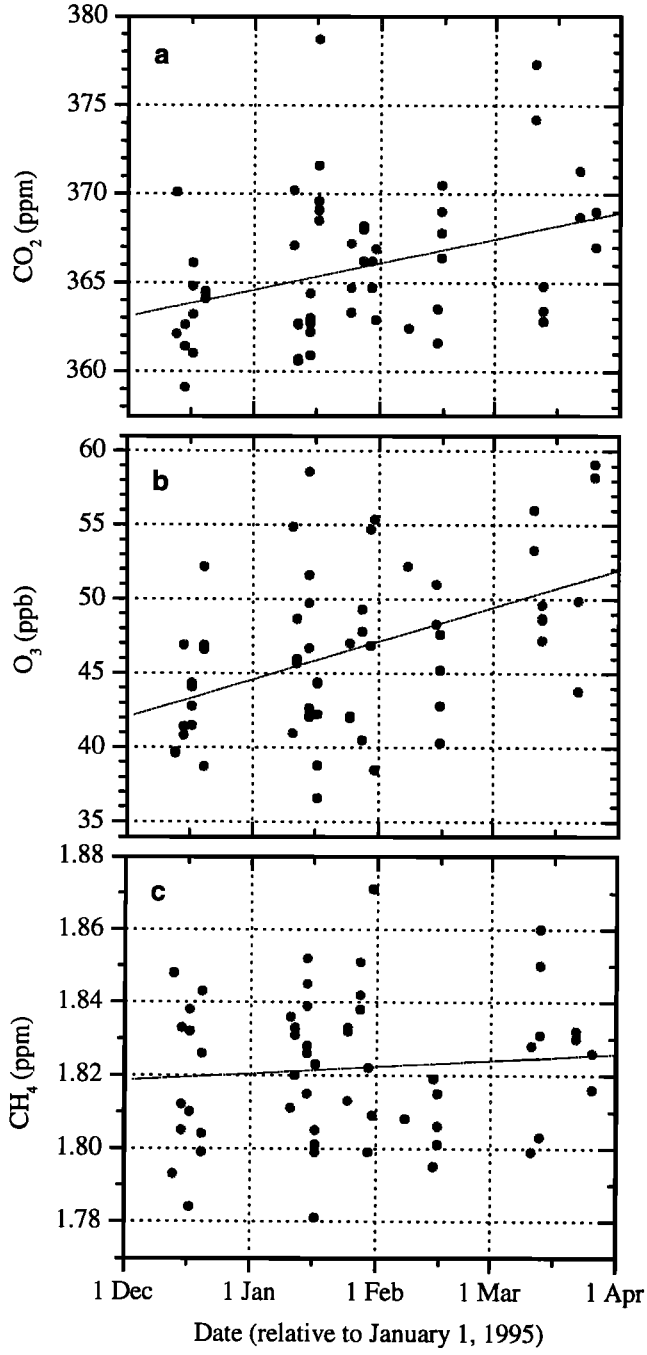

Figure 7. Seasonal behavior of (a) CO_2, (b) O_3, and (c) CH_4 in the upper troposphere, given relative to the January 1, 1995. The growth rates for CO_2 and SF_6 data were eliminated (see section 4.1.2).

Browell et al. [1992b] and *Oltmans* [1993], but the O_3 data presented in this section are restricted to the background troposphere. Ozone changes, for example, due to the increasing frequency of tropopause folds or due to the growing O_3 levels within them, both assumed to persist in the course of the northern winter [*VanHaver et al.*, 1996], are not considered here.

4.1.4. Trace gas correlations in the troposphere. Structures found in the meridional trace gas profiles already gave hints for three types of air masses

to be distinguished by their potential temperature at flight altitude (see section 4.1.2): arctic air ($\theta < 293$ K), polar air (293 K $< \theta <$ 300 K), and subtropical air ($\theta > 300$ K). That assumption is confirmed now since the trace gases are shown to correlate differently in these air masses (see Figure 8 and Table 3).

4.1.4.1. Correlations in arctic air ($\theta < 293$ K): CH_4 and SF_6 are positively correlated ($R = 0.52$, Figure 8d), whereas both species are negatively correlated to O_3 ($R = -0.51$ and -0.66; Figures 8a and 8b). This is probably because all sources of atmospheric CH_4 and SF_6 are located at the ground, but at least 50% of the polar upper tropospheric O_3 is injected from the stratosphere [*Browell et al.*, 1992a, 1994; *Gregory et al.*, 1992; *Mauzerall et al.*, 1996; *Oltmans*, 1993]. As the low and constant CO_2 levels of 364 ± 3 ppm point to clean air, we can conclude -1- that rapid upward movement from the ground is not likely to occur or is at least strongly suppressed by the high static stability of the wintertime arctic troposphere and -2- that the arctic upper troposphere is composed mainly of two types of air masses: well-mixed free tropospheric air from more southern latitudes (high CH_4 and SF_6 and low O_3) and stratospheric air (low CH_4 and SF_6 and high O_3).

CH_4, O_3, and SF_6 do not correlate significantly with CO_2. In contrast, a close relation between CO_2 and CH_4 was observed in the arctic troposphere by *Conway and Steele* [1989]. A similar but less pronounced correlation can be extracted from the present data when forming means for those flights for which at least three samples are available: January 25, 1994, January 28, 1994, March 13, 1994, January 12, 1995, and January 15, 1995 (large circles in Figure 8c). As illustrated by the straight line, CH_4 and CO_2 correlate linearly, whereas the slope of the correlation line of 3.5 ppb ppm^{-1} is much smaller than the 17 ppb ppm^{-1} determined by *Conway and Steele* [1989]. However, our data were gathered in midwinter, while *Conway and Steele* [1989] measured in April. During winter, both CO_2 and CH_4 vary modestly in the troposphere, but in April, CH_4 declines because of increasing tropospheric OH [*Dlugokencky et al.*, 1995]. Just in that time, CO_2 starts to decrease because of the beginning of plant assimilation. Therefore, and because of the simultaneous stronger latitudinal CH_4 gradient, the slope of the CH_4/CO_2 correlation line should actually be much larger in April than in the midwinter.

4.1.4.2. Correlations in polar air (293 K $< \theta <$ 300 K): Polar air shows a similar trace gas behavior as arctic air, but the trace gas correlations become more

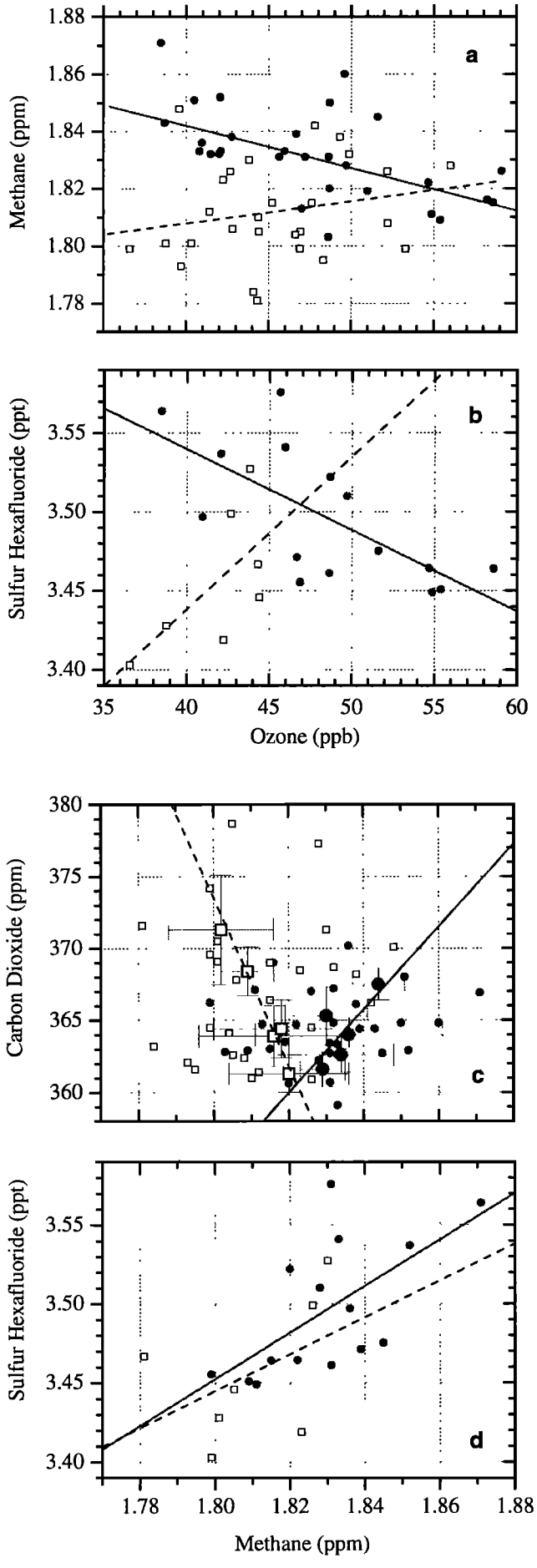

Figure 8. Correlations of **(a)** CH_4 versus O_3, **(b)** SF_6 versus O_3, **(c)** CO_2 versus CH_4, and **(d)** SF_6 versus CH_4 encompassing all tropospheric samples, dots and solid correlation lines for high-latitude air (polar and arctic air), open squares and dashed correlation line for subtropical air. See section 4.1.4 concerning the large squares and large dots.

compact, and O_3 varies more strongly. In our opinion these observations together point to the fact that polar air is more closely connected to its sources, i.e., is more frequently supplied by stratospheric air and by surface air. This can actually be expected because -1- isentropes crossing polar air can partly reach into the stratosphere [*Chen*, 1995; *Holton et al.*, 1995] and thus allow quasi-isentropic transport across the tropopause (the low O_3 observed at very high latitudes and theoretical studies by *Hoerling et al.* [1993] and *Siegmund et al.* [1996] suggest that this transport cycle is small north of ~65°N) and -2- the polar front and to a lesser extent the arctic front are known to cause strong vertical movement [*Shapiro et al.*, 1987] in which stratospheric air can reach the ground [*Elbern et al.*, 1997] and where tropospheric air can strongly be lifted up [*Ebel et al.*, 1996; *Grewe and Dameris*, 1995; *Juckes*, 1997; *Siegmund et al.*, 1996; *Van Velthoven and Kelder*, 1996].

4.1.4.3. Correlations in subtropical air ($\theta >$ 300 K): South of the polar front all trace gases correlate weakly and positively, though only the SF_6 - O_3 correlation seems to be definite ($R = 0.66$; p value = 0.15; 6 samples). Surprisingly, the negative correlations of O_3 versus CH_4 and SF_6 found in polar regions are not only reduced in midlatitudes but switch to the positive. Accordingly, the source partitioning of ozone has to exhibit a meridional change along the 400 hPa level. Two causes are probably responsible for this observation: -1- the 400 hPa level is located only 0.5-2 km below the tropopause in high latitudes but 2-5 km in midlatitudes, and -2- as already mentioned in section 4.1.2, polluted, i.e., CO_2- and probably NO_x- and O_3-enriched air, was frequently found south of $\phi = 50°$N. This suggests that a significant part of O_3 in the middle and upper midlatitude troposphere is lifted up from the ground.

A further change in the trace gas correlations was detected: CH_4 and CO_2 correlate negatively in subtropical air. Albeit this conclusion could already be derived from Figure 6 (CO_2 decreases with latitude whereas CH_4 increases), as in high latitudes, the correlation is only visible in Figure 8 when forming means of individual flights (open squares), here of December 17, 1994, December 20, 1994, February 15, 1994, February 16, 1994, and January 17, 1995. The slope of the correlation line of -1.7 ppb ppm^{-1} is slightly smaller compared to -2.2 ppb ppm^{-1} when using the CO_2 and CH_4 gradients between $\phi = 68°$ ($\theta = 297.5$ K) and 42°N (312.5 K) depicted in Figure 6 and listed in Table 2.

Likewise, a negative CH_4 - CO_2 correlation can be derived from airborne sampling above Russia by *Nakazawa et al.* [1997b]. When plotting the data given in their Table 2 for altitudes between 5 and 7.5 km, a significant anticorrelation ($R = -0.78$) showing a slope of -7.0 ppb ppm^{-1} can be inferred. Surprisingly, for their data originating from the planetary boundary layer, no correlation is present ($R < \pm 0.1$). Therefore mixing processes and long-range transport can lead to different tracer gas correlations in the upper troposphere than at the ground.

4.2. The Stratospheric Data

As addressed in section 3, stratospheric samples were identified by O_3 levels above the ozonopause value determined to 60 ppb. Although these samples were typically taken only 0-1.5 km above the tropopause (see Table 4), as shown below, their trace gas compositions behave differently from upper tropospheric air.

4.2.1. Vertical trace gas gradients in the lowermost stratosphere. First, a suitable flight parameter had to be found that describes most realistically how far the aircraft immersed into the stratosphere. As among samples 30-32, all stratospheric samples were collected within (mesoscale) tropopause folds or baroclinic zones; the use of (model-processed) meteorological data, for example, the ECMWF potential vorticity field, failed to determine the vertical distance of the aircraft to the tropopause accurately (note the scatter in Figure 2). Again, the (in situ measured) potential temperature was identified to be a reliable quantity (see Figure 9). The transition from tropospheric to stratospheric air is emphasized by distinguishing samples which trace gas composition shows an intermediate dependence on the potential temperature, namely, O_3 levels between 60 and 110 ppb. In the troposphere the trace gas vs. potential temperature relation describes meridional trace gas profiles (see Figure 6), but in the stratosphere the relation describes vertical trace gas profiles (see Figure 9). The vertical trace gas gradients for the intermediate range (stars) and the "pure" stratospheric samples (open circles) are quoted in Table 5 in which the potential temperature is used as a vertical coordinate. Note that this type of gradient is nearly conservative during rapid vertical displacement of the tropopause, which is not the case when using the altitude as a vertical coordinate.

As expected, O_3 strongly increases just above the tropopause, but its close dependence on the potential temperature, $R = 0.97$ for O_3 levels above 110 ppb, is somewhat surprising. The observed deviations from the linear relation are mainly due to variations of the potential temperature with latitude. Namely, the ozonopause shows a nearly constant potential temperature of 287 ± 2 K near the North Pole and around 305 K at ~50°N. Assessing this observation, note that each data point in Figure 9a represents a singular air mass arbitrarily picked out of a potpourri of strongly varying synoptical conditions and types of air masses.

A similar, close relationship to the potential temperature was seen for stratospheric methane (see Figure 9c and Table 5). For instance, considering the samples that show O_3 levels above 110 ppb, the correlation coefficient amounts to $R = -0.95$.

Unexpectedly, carbon dioxide strongly scatters between 358 and 372 ppm in the lowermost stratosphere (see Figure 9b). Because CO_2 in the extratropical over-

Table 4. Stratospheric Samples Characterized by O_3 Mixing Ratios Above 60 ppb

	Date	Time, GMT	φ, °N	ϑ, °E	T, °C	H, km	P, hPa	θ, K	TP km	O_3, ppb	CO_2, ppm	CH_4, ppm	SF_6, ppt
1	Jan. 25, 1994	10:27	76.2	3.5	−51.1	6.55	391	291.5	6.72	66.5	364.4	1.797	...
2	Jan. 28, 1994	13:52	54.2	9.3	−50.8	7.12	375	295.4	7.30	77.5	370.0	1.809	...
3	Jan. 28, 1994	14:28	51.3	9.5	−46.8	7.12	375	300.7	6.40	128.2	364.8	1.756	...
4	Feb. 15, 1994	13:19	85.0	9.6	−48.8	6.79	392	294.4	7.02	61.2	360.1	1.812	...
5	Feb. 15, 1994	15:00	77.8	10.9	−45.5	7.16	359	306.3	5.40	172.0	356.9	1.746	...
6	Mar. 11, 1994	16:45	65.8	25.5	−46.0	7.74	375	301.7	6.40	98.2	366.2	1.781	...
7	Mar. 16, 1994	16:35	64.5	1.8	−50.3	6.60	392	292.4	6.60	62.9	363.2	1.801	...
8	Mar. 16, 1994	18:39	56.7	−3.0	−48.2	6.99	376	298.7	6.11	104.2	363.2	1.775	...
9	Mar. 16, 1994	19:13	54.4	−0.2	−45.6	7.11	376	302.2	6.80	90.7	364.8	1.792	...
10	Dec. 13, 1994	10:49	56.4	15.6	−42.9	7.11	393	301.7	8.20	61.9	362.7	1.806	...
11	Dec. 13, 1994	12:31	61.8	17.7	−50.1	7.78	343	304.0	7.20	69.1	360.3	1.794	...
12	Dec. 20, 1994	14:06	59.4	−0.8	−48.1	7.18	376	298.8	7.18	97.6	365.6	1.767	...
13	Dec. 20, 1994	14:12	59.0	−0.4	−47.9	7.20	376	299.1	7.18	95.9	364.7	1.789	...
14	Dec. 20, 1994	15:52	52.0	6.4	−48.6	7.92	343	306.1	7.42	107.9	364.4	1.787	...
15	Dec. 20, 1994	16:05	51.3	7.5	−47.9	7.92	343	307.1	7.00	128.1	364.0	1.774	...
16	Jan. 11, 1995	09:00	51.4	9.7	−38.7	6.32	427	300.2	6.49	94.7	357.9	1.772	3.439
17	Jan. 11, 1995	09:13	52.1	9.8	−41.6	6.30	427	296.5	6.27	62.0	358.4	1.805	3.443
18	Jan. 11, 1995	12:38	65.5	12.0	−50.0	7.10	374	296.7	6.84	63.1	368.0	1.794	3.420
19	Jan. 31, 1995	07:48	61.5	25.6	−47.7	6.55	409	292.1	6.32	73.9	360.7	1.806	3.417
20	Jan. 31, 1995	08:02	60.4	25.1	−47.9	6.56	409	291.8	6.54	66.8	360.5	1.785	...
21	Jan. 31, 1995	08:55	57.1	23.4	−44.6	6.56	409	296.1	6.00	73.8	360.5	1.783	3.412
22	Feb. 3, 1995	10:47	71.8	22.0	−47.8	6.93	409	292.0	8.00	64.2	362.9	1.812	3.451
23	Feb. 3, 1995	11:06	72.8	23.7	−46.8	6.93	409	293.3	5.50	71.9	363.7	1.845	3.451
24	Feb. 3, 1995	11:41	74.4	28.2	−50.5	6.93	409	288.5	6.06	82.0	363.0	1.834	3.490
25	Feb. 3, 1995	12:16	75.1	37.1	−50.0	6.82	415	287.9	5.64	90.1	361.1	1.801	3.369
26	Feb. 3, 1995	12:24	74.9	39.3	−51.1	6.82	415	286.5	5.68	81.7	362.0	1.805	...
27	Feb. 5, 1995	11:18	74.7	40.2	−44.3	6.18	417	295.1	6.32	114.5	362.1	1.792	3.307
28	Feb. 5, 1995	11:24	74.5	41.6	−43.6	6.18	417	296.0	6.22	147.2	363.3	1.769	3.260
29	Feb. 5, 1995	11:28	74.4	42.5	−44.0	6.18	417	295.5	6.15	146.0	364.4	1.782	3.250
30	Feb. 9, 1995	13:09	70.0	23.4	−64.8	11.42	178	342.7	8.32	377.0	...	...	3.014
31	Feb. 21, 1995	13:03	67.9	19.2	−48.9	11.83	178	368.8	7.05	430.0	...	...	2.907
32	Feb. 21, 1995	13:13	67.7	17.4	−49.9	10.30	238	337.8	7.14	369.0	359.4	1.663	3.017
33	Mar. 26, 1995	16:46	73.0	30.0	−52.1	6.86	374	293.9	8.44	62.6	366.9	1.852	3.571
34	Mar. 26, 1995	19:19	70.9	18.4	−54.2	6.84	374	291.1	7.14	63.8	367.8	1.811	...
35	Mar. 26, 1995	19:55	69.7	19.0	−52.9	6.84	374	292.9	6.70	76.8	368.9	1.802	...
36	Mar. 26, 1995	19:59	69.4	19.2	−53.3	6.84	374	292.3	6.40	75.6	366.5	1.809	...
37	Mar. 26, 1995	20:07	68.8	19.6	−52.2	6.83	374	293.8	6.22	81.0	366.2	1.820	...
38	Mar. 27, 1995	15:36	62.0	5.5	−51.9	6.85	376	293.6	6.33	95.1	361.8	1.781	3.499
39	Mar. 27, 1995	15:47	61.3	5.1	−52.0	6.89	376	293.5	6.33	118.6	361.4	1.788	3.492
40	Mar. 27, 1995	16:22	58.3	5.6	−50.2	6.95	376	295.9	6.66	119.7	361.0	1.778	3.438
41	Mar. 27, 1995	17:24	54.3	9.8	−50.3	7.01	374	296.2	6.39	114.7	364.1	1.777	3.445
42	Mar. 27, 1995	17:28	54.0	9.8	−49.4	7.01	374	297.4	6.35	147.8	360.4	1.771	3.365
43	Mar. 27, 1995	17:49	52.3	10.0	−47.1	7.03	374	300.4	5.71	162.4	369.9	1.762	3.390
44	Mar. 27, 1995	17:55	51.9	10.1	−47.1	7.05	374	300.5	5.57	145.3	369.2	1.769	3.386
45	Mar. 27, 1995	17:59	51.6	10.1	−44.8	7.06	374	303.5	5.46	195.2	367.2	1.758	3.277
46	Mar. 27, 1995	18:04	51.3	10.1	−47.1	7.06	374	300.5	5.39	177.9	367.0	1.756	3.358
47	Mar. 27, 1995	18:21	50.1	10.2	−44.1	7.10	374	304.5	5.30	161.5	367.7	1.768	3.351
48	Apr. 4, 1995	16:15	59.2	10.3	−37.8	6.40	426	301.5	4.60	123.5	364.9	1.772	3.407
49	Apr. 4, 1995	16:18	59.4	10.3	−39.5	6.39	426	299.3	4.64	123.9	367.2	1.783	3.430
50	Apr. 4, 1995	18:23	66.0	15.7	−50.3	7.02	376	295.8	6.87	102.7	365.4	1.784	3.399
51	Apr. 4, 1995	18:38	66.7	17.3	−51.6	6.99	376	294.1	6.66	92.4	364.2	1.801	3.470
52	Apr. 4, 1995	18:54	67.4	19.3	−51.8	6.98	376	293.8	6.66	97.7	364.5	1.796	3.492
53	Apr. 5, 1995	20:15	75.7	29.9	−51.1	7.24	375	295.0	6.68	109.4	365.6	1.786	3.435
54	Apr. 5, 1995	20:31	74.6	30.0	−53.6	7.24	375	291.7	7.01	91.2	363.1	1.793	3.460
55	Apr. 8, 1995	06:19	61.4	17.3	−49.0	7.44	358	301.7	7.76	169.8	365.6	1.760	3.316
56	Apr. 8, 1995	06:53	59.3	15.4	−47.3	7.46	358	304.0	6.80	161.6	363.2	1.766	3.340
57	Apr. 8, 1995	07:18	57.6	13.9	−47.3	7.45	358	304.0	6.45	179.6	363.3	1.755	3.306
58	Apr. 8, 1995	07:22	57.4	13.6	−47.0	7.46	358	304.4	6.27	159.2	364.0	1.760	3.347
59	Apr. 8, 1995	09:02	49.4	10.3	−43.8	7.97	344	312.4	8.15	223.4	366.0	1.736	3.264
60	Apr. 8, 1995	09:07	49.1	10.6	−44.1	7.96	344	312.0	7.70	197.5	365.5	1.737	3.295
	Mar. 1		62.9	16.0	−48.0	6.99	383	297.5	6.51	109.1	364.1	1.786	3.357

The abbreviations are defined as follows: φ and ϑ, latitude and longitude of sampling; T, temperature; H, altitude; P, pressure; θ, potential temperature; and TP, height of the dynamical tropopause. Last row: mean of all samples (except sample 22), whereas the CO_2 and SF_6 data were adjusted to January 1, 1995 values (see section 4.1.2).

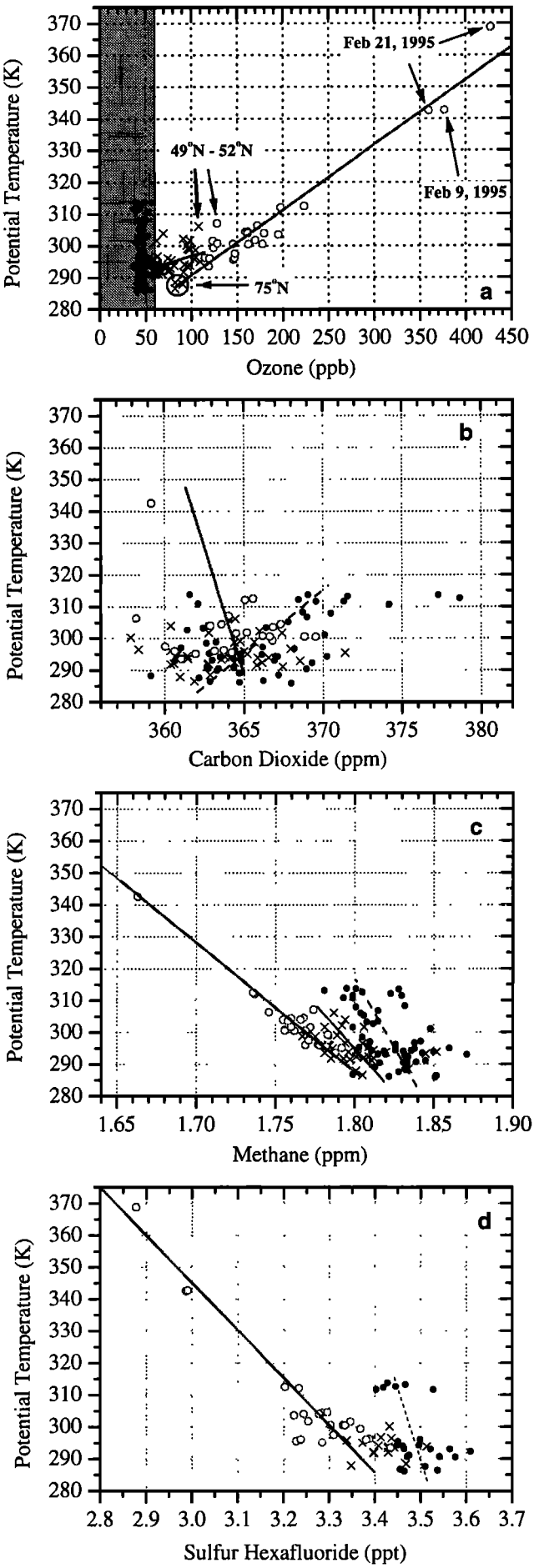

world is known to vary weakly [*Nakazawa et al.*, 1995; *Schmidt and Khedim*, 1991], our data obviously confirm that tropospheric air (which is subjected to pronounced CO_2 seasonality) is transported across the extratropical tropopause into the lowermost stratosphere. The vertical extension of this mixing area above the tropopause is estimated to be at least 2 km, on the basis of the strong scatter of CO_2 observed 1-2 km above the ozonopause. Why were only modest CO_2 variations below 5 ppm found in the lowermost stratosphere in all other aircraft observations such as those by *Nakazawa et al.* [1991] or *Strahan et al.* [1998]? The cause is probably found in the fact that all of our stratospheric samples were collected (besides the samples 30-32) in tropopause folds associated with the polar and arctic front. The other available data sets were gathered predominantly south of the polar front. Our measurements therefore suggest that troposphere-to-stratosphere transport efficiently occurs near the polar and arctic jet stream. Note, it has not been established until now, if similar considerable troposphere-to-stratosphere transport takes place further south near the subtropical jet stream. The strong phase shift in the CO_2 seasonality between the upper subtropical troposphere and the lowermost stratosphere observed by *Strahan et al.* [1998] at potential temperatures around 340 K seems to indicate that isentropic troposphere-to-stratosphere flux near the subtropical front is of minor importance.

Similar to CH_4, SF_6 decreases in the stratosphere (see Figure 9d). In this case, however, the vertical decrease is not caused by chemical degradation but rather by the strong tropospheric SF_6 increase of about 6.9% per year [*Geller et al.*, 1997; *Maiss et al.*, 1996] and the growing age of stratospheric air with increasing altitudes [*Harnisch et al.*, 1996, 1998; *Patra et al.*, 1997]. According to the latter authors, stratospheric SF_6 data make it possible to infer the residence time of air masses since their entry into the stratosphere (see next section).

4.2.2. Trace gas correlations in the lowermost stratosphere. In Figure 10, SF_6, CH_4, and CO_2 are plotted against O_3, and SF_6 is plotted against CH_4 distinguished in tropospheric and stratospheric air masses; the linear correlation coefficients R derived for both data sets are summarized in Table 3. As in the arctic troposphere, in the lowermost stratosphere, CH_4 and SF_6 (both emitted in the troposphere) are highly anticorrelated (correlation coefficients $R < -0.87$ and $R = -0.94$) to O_3 (being produced in the stratosphere). CO_2 scatters strongly above the tropopause and correlates weakly with O_3, CH_4, and SF_6. As outli-

Figure 9. All data versus the potential temperature during sampling for **(a)** O_3, **(b)** CO_2, **(c)** CH_4, and **(d)** SF_6. Open circles and solid regression lines indicate stratospheric samples showing O_3 levels beyond 110 ppb. Stars indicate stratospheric samples showing O_3 levels of 60-110 ppb. Dots and dashed regression lines indicate tropospheric samples.

Table 5. Linear Correlation Coefficient and Vertical Gradient of O_3, CO_2, CH_4, and SF_6 Within the Lowermost Stratosphere Using the Potential Temperature As Vertical Coordinate

	Linear Correlation Coefficient		Vertical Gradient
	$O_3 = (60 - 110)$ ppb	$O_3 > 110$ ppb	
O_3	0.29 (0.09)	0.97 (0.00)	4.9 ppb K^{-1}
CO_2	$< \pm 0.1$	−0.21 (0.33)	−0.062 ppm K^{-1}
CH_4	−0.44 (0.01)	−0.95 (0.00)	−2.5 ppb K^{-1}
SF_6	$< \pm 0.1$	−0.93 (0.00)	−0.0067 ppt K^{-1}

See Figure 9. The p values, the probability that the linear correlation coefficient R is zero, are given in parentheses.

ned in section 4.2.1, this observation points to intensive troposphere-to-stratosphere transport in the vicinity of polar and arctic tropopause folds.

Because of the well-defined ozonopause of 60 ppb (see Figure 2) and the close relation between SF_6 and O_3 ($R = 0.94$; see Figure 10a), we are able to infer the mean SF_6 mixing ratio at the entry of tropospheric air into the lowermost stratosphere. Since all SF_6 data are adjusted to January 1, 1995 values, the derived value of $SF_6(TP) = 3.457$ ppt is only valid for that date. Using $SF_6(TP)$ and the SF_6 growth rate of 6.9% yr^{-1} in late 1994 [*Geller et al.*, 1997; *Maiss et al.*, 1996], we can derive the stratospheric residence time of each examined air parcel (see Figure 11). The calculated SF_6 ages are rather high, i.e., 2-2.5 years, only 3.5 km above the tropopause. However, note also that in the literature the interpretation of tracer ages compared to generally lower stratospheric turnover times is controversial [*Appenzeller et al.*, 1996b; *Boering et al.*, 1996; *Daniel et al.*, 1996; *Harnisch et al.*, 1998; *Hall and Plumb*, 1994; *Pollock et al.*, 1992; *Rosenlof*, 1995; *Schmidt and Khedim*, 1991; *Woodbridge et al.*, 1995; *Yang and Tung*, 1996]. To assess the inferred SF_6 ages, one has to take the following aspects in consideration.

1. The major part of the troposphere-to-stratosphere flow takes place in the tropics [*Holton et al.*, 1995], where the SF_6 levels are lower compared to high latitudes [*Geller et al.*, 1997; *Maiss et al.*, 1996]. Referring our data to a modified value using $SF_6(TP) = 3.342$ ppt calculated with the reference function at Mauna Loa $(0.004172 \cdot (t - 1966.694)^2$ using t = 1995 = January 1, 1995) given by *Harnisch et al.* [1998], the calculated SF_6 ages are ~0.6 years lower (see second y scale in Figure 11).

2. There are many experimental and theoretical indications that extratropical troposphere-to-stratosphere transport is a frequent phenomenon [*Chen*, 1995; *Dessler et al.*, 1995; *Hoerling et al.*, 1993; *Juckes*, 1997; *Mote et al.*, 1994; *Holton et al.*, 1995; *Siegmund et al.*, 1996; *Zahn et al.*, 1998a]. At first glance this assumption is supported by the observed closely linear SF_6-O_3 relation and the continuous transition into the (extratropical) stratosphere. If the major SF_6 source to the stratosphere was different from the extratropical tropopause, deeper in a (chemically undisturbed) stratosphere, one would expect an increasing deviation from the correlation line obtained directly above the tropopause. This was not observed.

3. Because of diabatic cooling and descent of air masses in the polar vortex and its good isolation from the surrounding surf zone, polar vortex air was shown to be much older than ex-vortex air [*Daniel et al.*, 1996; *Harnisch et al.*, 1996; *Waugh et al.*, 1997].

In any case, the observational fact is that depending on the actual partitioning of the tropical and the extratropical troposphere-to-stratosphere fluxes, the SF_6 age of the air parcels examined around 11 km and showing O_3 levels of ~400 ppb (samples 30-32) amounted roughly to 2 years. This is much older than was inferred by most of the other investigations listed above but agrees excellently with results from a balloon-borne SF_6 profile on March 7, 1995, only 2 weeks after our flights and at exactly the same location (Kiruna, Sweden; 68°N, 20°E) [*Harnisch et al.*, 1996]. Further information is given by the experiments additionally installed aboard our Cessna aircraft (note, only samples 30-32 were collected onboard the high-flying Cessna aircraft; see section 2): (1) Both air parcels sampled on February 9, 1995 (sample 30) and on February 21, 1995 (samples 31 and 32), were beneath the polar vortex. (2) The observed O_3 levels were atypically low. (3) The total reactive nitrogen NO_y (mainly NO, NO_2, HNO_3, $ClONO_2$, N_2O_5, and HONO) was severely elevated, up to a factor of 6 [*Fischer et al.*, 1997]. These observations were explained by strong subsidence of O_3-depleted and NO_y-enriched vortex air during this winter and by nitrification of the lowermost stratosphere associated with sedimentation and following evaporation of HNO_3 carrying polar stratospheric cloud (PSC) particles. The "subsidence hypothesis" is supported by our SF_6 measurements pointing to air parcel ages which are a factor 2−3 higher than typically encountered in the lowermost stratosphere. Therefore, and because of the depleted O_3, the hypothesis that the intensive influx of tropos-

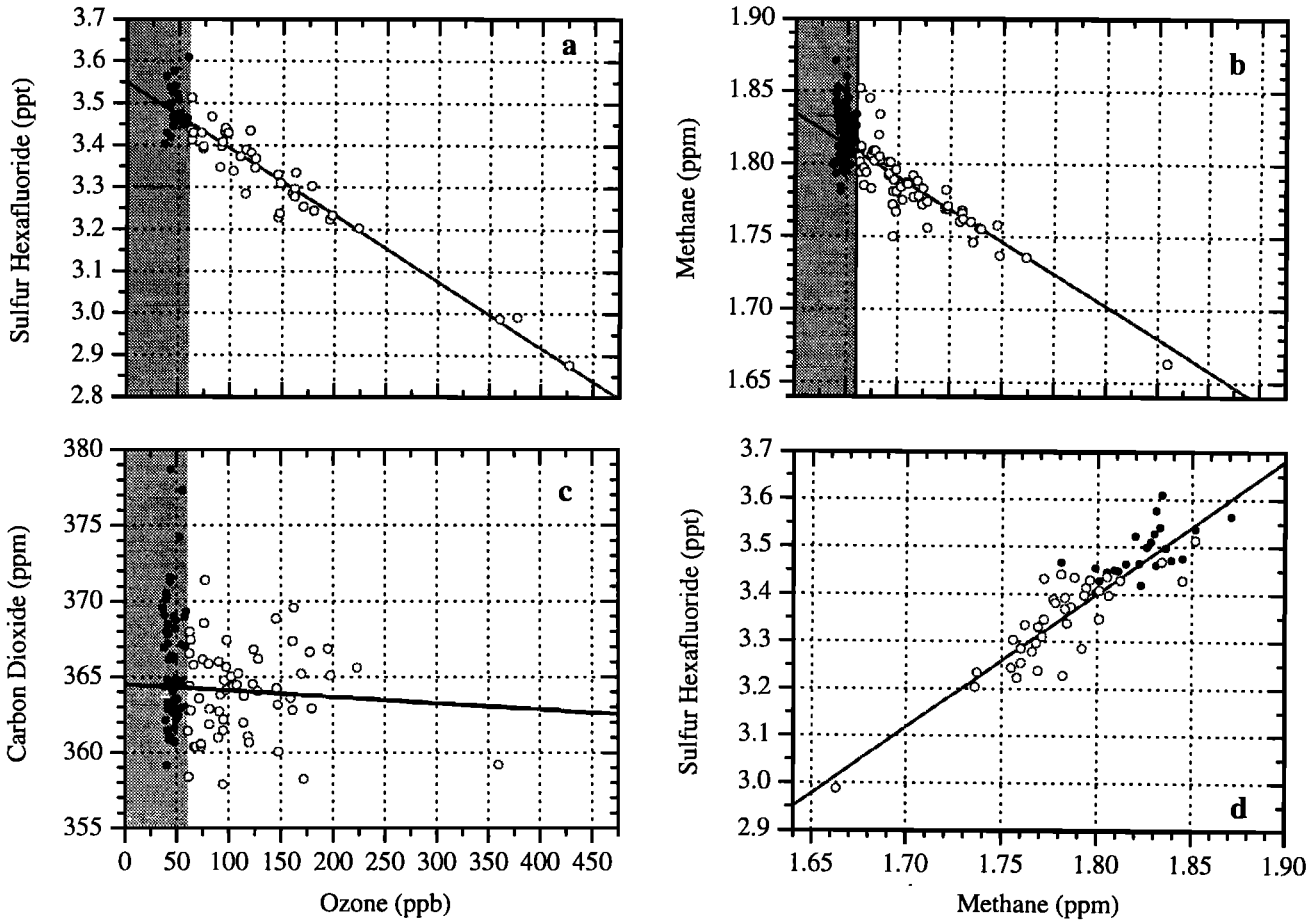

Figure 10. Correlations of **(a)** SF_6 versus O_3, **(b)** CH_4 versus O_3, **(c)** CO_2 versus O_3, and **(d)** SF_6 versus CH_4 for the stratospheric samples. See Table 3 for correlation coefficients.

pheric air traced by the samples collected just above the ozonopause (see section 4.2.1) influences the trace gas composition deeper in the lowermost stratosphere and causes the detected linear SF_6-O_3 relation is suspicious.

5. Summary and Concluding Remarks

Although our data set embraces only individual air mass samples out of a large flight area and time interval, a consistent picture of the property of upper tro-

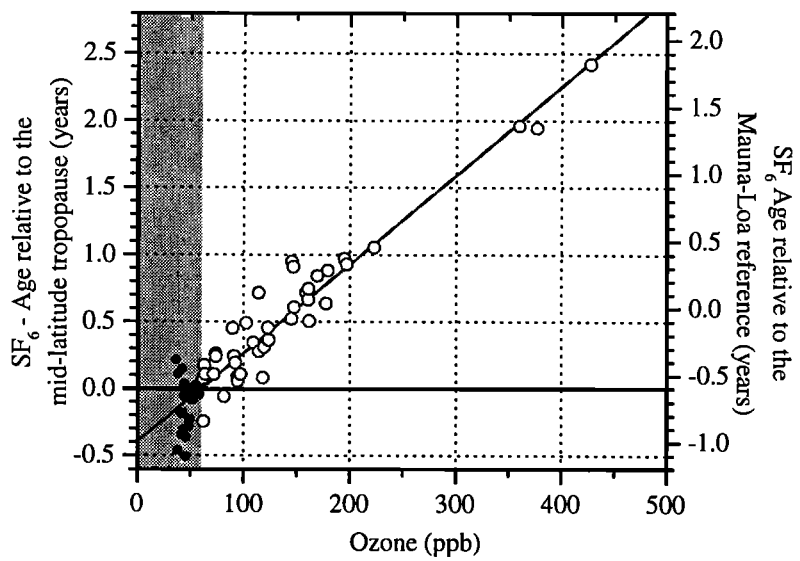

Figure 11. SF_6 age for each air mass examined. The SF_6 mixing ratio at the extratropical tropopause is set to 3.457 ppt (left y axis) or to 3.342 ppt calculated with the reference function at Mouna Loa given by *Harnish et al.* [1998] (right y axis, see section 4.2.2).

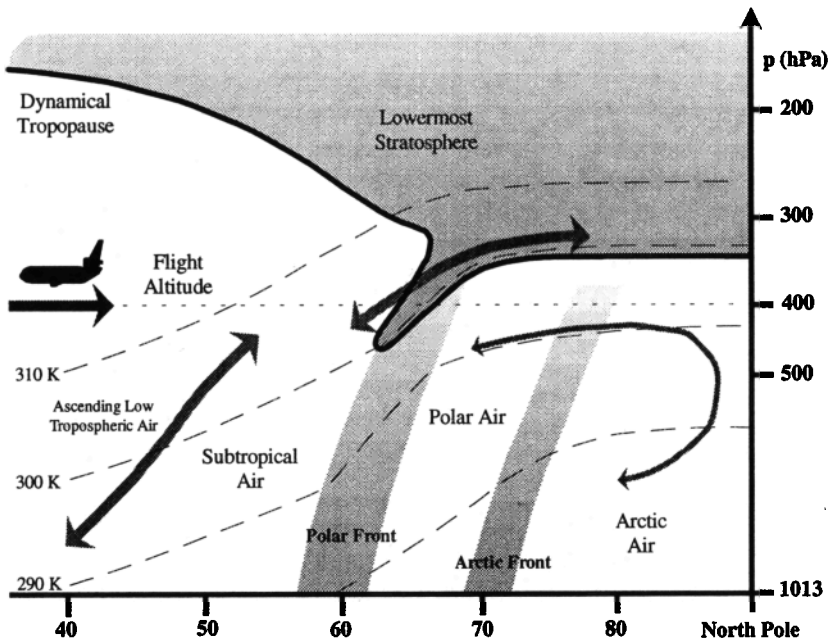

Figure 12. Schematic picture displaying the different air masses and the transport phenomena identified along the 400 hPa level. Shaded arrows indicate transport stream lines. Dashed lines indicate isentropes. Particularly in the low troposphere, ascending air mostly crosses isentropes because of (diabatic) heating during cloud formation. The amount of stratospheric O_3 at 400 hPa is likely the highest around the polar front because, first, the stratospheric O_3 influx is intensive and, second, the 400 hPa level is close to the tropopause. The latter condition is not fulfilled south of the polar front, where the stratospheric O_3 ingress can also be high. North of the polar front, insignificant isentropic cross-tropopause flux occurs because of the nearly parallel alignment of the tropopause and the isentropes.

pospheric air north of 40°N could be extracted. With the help of 7-day back trajectories the potential temperature of a tropospheric air parcel was shown to trace excellently the mean latitude the air parcel spent the last week before examination. On the basis of this finding we propose that the potential temperature should be more frequently utilized to create representative meridional trace gas distributions in the troposphere, comparable as done here by introducing the representative latitude. For instance, the 300 K isentrope was found to mark the polar front in the upper troposphere and thus was identified as the lowest isentrope allowing quasi-adiabatic cross-tropopause flux. Furthermore, categorizing our data with help of the potential temperature θ together with inferred meridional varying trace gas correlations made it possible to distinguish subtropical air ($\theta > 300\,K$), polar air ($\theta = 293 - 300\,K$), and arctic air ($\theta = 286 - 293\,K$) at 400 hPa. In addition, the impressing compact correlation of the potential temperature with O_3, CH_4, and SF_6 just above the ozonopause suggests that near the mid-latitude and high-latitude tropopause (which strongly varies in space and time) and in the very lowermost stratosphere, the potential temperature can be a reliable measure for the vertical distance above the tropopause (see Figure 9).

In Figure 12 we attempt to summarize our findings in the form of a schematic sketch. The transition from subtropical to polar air is maintained by the strongly baroclinic polar front. Owing to smaller presence and weaker baroclinity of the arctic front [*Shapiro et al.*, 1987], the transition from polar to arctic air is much more continuous and permeable than at the polar front (the mean location of both frontal zones at 64°N ($\theta = 300$ K) and 76°N ($\theta = 293$ K) is only based on our wintertime observations at ~400 hPa).

The largest influx of stratospheric air takes place presumably around the polar frontal zone since the highest O_3 concentrations were observed there. As illustrated by the shaded arrows, this stratospheric air is subsequently mixed with surrounding subtropical and polar air. North of ~70°N, injection of stratospheric air seems to be of minor importance as the observed O_3 level was low, although the tropopause was located, on average, only 700 m above the aircraft. Elevated CO_2 levels and trajectory calculations reveal that the midlatitude middle and upper troposphere are significantly influenced by upward traveling surface air that starts from different areas in the subtropics and midlatitudes. This assumption is confirmed by the observation that O_3 represents a tracer of stratospheric air in the polar troposphere but a tracer of polluted air in midlatitudes. Clear signs of anthropogenic pollution were not found

north of ~65°N, implying that the arctic upper troposphere is mainly supplied with northward traveling polar air.

Strongly varying CO_2 mixing ratios found just above the ozonopause suggest that at least the lowest part of the mid-latitude and high-latitude lowermost stratosphere is strongly affected by mixing with tropospheric air entering the stratosphere near the polar front. This cross-tropopause flux of tropospheric air might be stronger than that near the subtropical jet at corresponding higher potential temperatures in the 340-360 K range, as, e.g., observed by *Bregman et al.* [1997] and *Hintsa et al.* [1998]. The high SF_6 age encountered in the arctic lowermost stratosphere, 2 years around 11 km (3 km above the tropopause), lets us assume that because of the strong polar vortex in the winter 1994-1995, a considerable amount of vortex air has flown out at its bottom (~ 380 K) and was continuously mixed with surrounding exvortex air.

Acknowledgments. This work was supported by the BMBF under grant 01LO9532. Additional financial support from the EU is highly appreciated (grant EV5V CT93-0341). ECMWF is thanked for the provision of their meteorological analyses and M. Bolder (Wageningen University, Netherlands) is thanked for taking three glass flask samples aboard the Cessna Citation aircraft in February 1995. We thank particularly one of the reviewers for his excellent and comprehensive comments.

References

Anderson, B.E., G.L. Gregory, J.E. Collins Jr., G.W. Sachse, T.J. Conway, and G.P. Whiting, Airborne observations of spatial and temporal variability of tropospheric carbon dioxide, *J. Geophys. Res., 101*, 1985-1997, 1996.

Appenzeller, C., H.C. Davies, and W.A. Norton, Fragmentation of stratospheric intrusions, *J. Geophys. Res., 101*, 1435-1456, 1996a.

Appenzeller, C., J.R. Holton, and K.H. Rosenlof, Seasonal variation of mass transport across the tropopause, *J. Geophys. Res., 101*, 15,071-15,078, 1996b.

Arnold, F., J. Schneider, K. Gollinger, H. Schlager, P. Schulte, D.E. Hagen, P.D. Whitefield, and P. van Velthoven, Observation of upper tropospheric sulfur dioxide- and acetone-pollution: potential implications for hydroxyl radical and aerosol formation, *Geophys. Res. Lett., 24*, 57-60, 1997.

Beekmann, M., et al., Regional and global tropopause fold occurence and related ozone flux across the tropopause, *J. Atmos. Chem., 28*, 29-44, 1997.

Bergren, R., The distribution of temperature and wind connected with active tropical air in the higher troposphere and with some remarks concerning clear air turbulence at high altitudes, *Tellus, 4*, 43-53, 1952.

Bethan, S., G. Vaughan, and S.J. Reid, A comparison of ozone and thermal tropopause heights and the impact of tropopause definitions on quantifying the ozone content of the troposphere, *Q.J.R. Meteorol. Soc., 122*, 929-944, 1996.

Boering, K.A., S.C. Wofsky, B.C. Daube, H.R. Schneider, M. Loewenstein, J.R. Podolske, and T.J. Conway, Stratospheric mean ages and transport rates from observations of carbon dioxide and nitrous oxide, *Science, 274*, 1340-1343, 1996.

Bolin, B., and W. Bischof, Variations of the carbon dioxide content of the atmosphere in the northern hemisphere, *Tellus, 22*, 431-442, 1970.

Borrmann, S., S. Solomon, J.E. Dye, and B. Luo, The potential of cirrus clouds for heterogeneous chlorine activation, *Geophys. Res. Lett., 23*, 2133-2136, 1996.

Brasseur, G.P., and S. Solomon, *Aeronomy of the Middle Atmosphere*, D. Reidel, Norwell, Mass., 1986.

Bregman, A., P.F.J. van Velthoven, F.G. Wienhold, A. Waibel, T. Zenker, A. Frenzel, M.J.A. Bolder, G.H. Harris, F. Arnold, and J. Lelieveld, Aircraft measurements of O_3, HNO_3, and N_2O in the winter arctic lower stratosphere during the Stratosphere-Troposphere Experiment by Aircraft Measurements (STREAM), *J. Geophys. Res., 100*, 11,245-11,260, 1995.

Bregman, A., et al., In situ trace gas and particle measurements in the summer lower stratosphere during STREAM II: Implications for O_3 production, *J. Atmos. Chem., 26*, 275-310, 1997.

Browell, E.V., E.F. Danielsen, S. Ismail, G.L. Gregory, S.M. Beck, Tropopause fold structure determined from airborne lidar and in-situ measurements, *J. Geophys. Res., 92*, 2112-2120, 1987.

Browell, E.V., C.F. Butler, S.A. Kool, M.A. Fenn, R.C. Harriss, and G.L. Gregory, Large-scale variability of ozone and aerosols in the summertime Arctic and Subarctic troposphere, *J. Geophys. Res., 97*, 16,433-16,450, 1992a.

Browell, E.V., C.F. Butler, M.A. Fenn, S.A. Kooi, and W.B. Grant, Tropospheric ozone and aerosol variability observed at high northern latitudes with an airborne lidar, Proceedings of the 1992 Quadrennial Ozone Symposium, Charlottesville, 4-13 June, 1992b.

Browell, E.V., M.A. Fenn, C.F. Butler, W.B. Grant, R.C. Harriss, and M.C. Shipham, Ozone and aerosol distributions in the summertime troposphere over Canada, *J. Geophys. Res., 99*, 1739-1755, 1994.

Chen, P., Isentropic cross-tropopause mass exchange in the extratropics, *J. Geophys. Res., 100*, 16,661-16,673, 1995.

Conway, T.J., and L.P. Steele, Carbon dioxide and methane in the arctic atmosphere, *J. Atmos. Chem., 9*, 81-99, 1989.

Conway, T.J., P.P. Tans, L.S. Waterman, K.W. Thoning, K.A. Masarie, and R.H. Gammon, Atmospheric carbon dioxide measurements in the remote global troposphrere, 1981-1984, *Tellus, 40, Ser. B*, 81-115, 1988.

Conway, T.J., P.P. Tans, L.S. Waterman, K.W. Thoning, D.R. Kitzis,, K.A. Masarie, and N. Zhang, Evidence for interanuual variability of the carbon cycle from the National Oceanic and Atmospheric/Climate Monotoring and Diagnostic Laboratory Global Air Sampling Network, *J. Geophys. Res., 99*, 22,831-22,855, 1994.

Crutzen, P., On the role of CH_4 in atmospheric chemistry: Sources, sinks and possible reductions in anthropogenic sources, *Ambio, 24*, 52-55, 1995.

Daniel, J.S., S.M. Schauffler, W.H. Pollock, S. Solomon, A. Weaver, L.E. Heidt, P.R. Garcia, E.L. Atlas, and J.F. Vedder, On the age of stratosperic air and inorganic chlorine and bromine release, *J. Geophys. Res., 101*, 16,757-16,770, 1996.

Danielsen, E.F., Stratospheric-Tropospheric Exchange based on radioactivity, ozone and potential vorticity, *J. Atmos. Sci., 25*, 502-518, 1968.

Danielsen, E.F., and V.A. Mohnen, Project Duststorm Report: Ozone transport, in situ measurements and meteorological analyses of tropopause foldings, *J. Geophys. Res., 82*, 5867-5877, 1977.

Denning, A.S., I.Y. Fung, and D. Randall, Latitudinal gradient of atmospheric CO_2 due to seasonal exchange with land biota, *Nature, 376*, 240-243, 1995.

Dessler, A.E., E.M. Weinstock, J.G. Anderson, and K.R.

Chan, Mechanisms controlling water vapor in the lower stratosphere: A tale of two stratospheres, *J. Geophys. Res.*, *100*, 23,167-23,172, 1995.

Dlugokencky, E.J., L.P. Steele, P.M. Lang, and K.A. Masarie, The growth rate and distribution of atmospheric methane, *J. Geophys. Res.*, *99*, 17,021-17,043, 1994.

Dlugokencky, E.J., L.P. Steele, P.M. Lang, and K.A. Masarie, Atmospheric methane at Mauna Loa and Barrow observatories: presentation and analysis of in situ measurements, *J. Geophys. Res.*, *100*, 23,103-23,113, 1995.

Ebel, A., H. Elbern, J. Hendricks, and R. Meyer, Stratosphere-troposphere exchange and its impact on the structure of the lower stratosphere, *J. Geomagn. Geoelectr.*, *46*, 135-144, 1996.

Elbern, H., J. Kowol, R. Sladkovic, and A. Ebel, Deep stratospheric intrusions: a statistical assessment with model guided analyses, *Atmos. Environ.*, *31*, 3207-3226, 1997.

Fischer, H., A.E. Waibel, M. Welling, F.G. Wienhold, T. Zenker, P.J. Crutzen, F. Arnold, V. Bürger, J. Schneider, A. Bregman, J. Lelieveld, and P.C. Siegmund, Observations of high concentrations of total reactive nitrogen (NO_y) and nitric acid (HNO_3) in the lower arctic stratosphere during the Stratosphere-Troposphere Experiment by aircarft measurements (STREAM) II campaign in February 1995, *J. Geophys. Res.*, *102*, 23,559-23,571, 1997.

Fung, I., J. John, J. Lerner, E. Matthews, M. Prather, L.P. Steele, and P.J. Fraser, Three-dimensional model synthesis of the global methane cycle, *J. Geophys. Res.*, *96*, 13,033-13,065, 1991.

Geller, L.S., J.W. Elkins, J.M. Lobert, A.D. Clarke, D.F. Hurst, J.H. Butler, and R.C. Myers, Tropospheric SF_6: Observed latitudinal distribution and trends, derived emissions and interhemispheric exchange time, *Geophys. Res. Lett.*, *34*, 675-678, 1997.

Gemery, P.A., M. Trolier, and J.W.C. White, Oxygen isotope exchange between carbon dioxide and water following atmospheric sampling using glass flasks, *J. Geophys. Res.*, *101*, 14,415-14,420, 1996.

Gregory, D.R., B.E. Anderson, L.S. Warren, E.V. Browell, D.R. Bagwell, and C.H. Hudgins, Tropospheric ozone and aerosol observations: The Alaskan Arctic, *J. Geophys. Res.*, *97*, 16,451-16,471, 1992.

Grewe, V., and M. Dameris, Calculating the global mass exchange between stratosphere and troposphere, *Ann. Geophysicae*, *14*, 431-442, 1996.

Hall, T.M., and R.A. Plumb, Age as a diagnostic of stratospheric transport, *J. Geophys. Res.*, *99*, 1059-1070, 1994.

Harnisch, J., R. Borchers, P. Fabian, and M. Maiss, Tropospheric trends for CF_4 and C_2F_6 since 1982 derived from SF_6 dated stratospheric air, *Geophys. Res. Lett.*, *23*, 1099-1102, 1996.

Harnisch, J., W. Bischof, R. Borchers, P. Fabian, and M. Maiss, A stratospheric excess of CO_2 - due to tropical deep convection, *Geophys. Res. Lett.*, *25*, 63-66, 1998.

Harnish, J., and A. Eisenhauer, Natural CF_4 and SF_6 on Earth, *Geophys. Res. Lett.*, *25*, 2401-2404, 1998.

Haynes, P.H., C.J. Marks, M.E. McIntyre, T.G. Sheperd, and K.P. Shine, On the 'downward control' of the extratropical diabatic circulations by eddy-induced mean zonal forces, *J. Atmos. Sci.*, *48*, 651-678, 1991.

Heidt, L.E., J.P. Krasnec, R.A. Lueb, W.H. Pollock, B.E. Henry, and P.J. Crutzen, Latitudinal distribution of CO and CH_4 over the Pacific, *J. Geophys. Res.*, *85*, 7329-7336, 1980.

Held, I.M., On the height of the tropopause and the static stability of the tropopause, *J. Atmos. Sci.*, *39*, 412-417, 1982.

Hintsa, E.J., et al., Troposphere-to-stratosphere transport in the lowermost stratosphere from measurements of H_2O, CO_2, N_2O and O_3, *Geophys. Res. Lett.*, *25*, 2655-2658, 1998.

Hoerling, M.P., T.K. Schaack, and A.J. Lenzen, A global analysis of stratospheric-tropospheric exchange during northern winter, *Mon. Weather Rev.*, *121*, 162-172, 1993.

Holton, J.R., P.H. Haynes, M.E. McIntyre, A.R. Douglass, R.B. Rodd, and L. Pfister, Stratosphere-troposphere exchange, *Rev. Geophys.*, *33*, 403-439, 1995.

Hoskins, B.J., Towards a PV-theta view of the general circulation, *Tellus*, *43*, *Ser. AB*, 27-35, 1991.

Hoskins, B.J., M.E. McIntyre, A.W. Robertson, On the use and significance of isentropic potential vorticity maps, *Q.J.R. Meteorol. Soc.*, *111*, 877-946, 1985.

Jacob, D.J., M.J. Prather, S.C. Wofsky, and M.B. McElroy, Atmospheric distribution of ^{85}Kr simulated with a general circulation model, *J. Geophys. Res.*, *92*, 6614-6626, 1987.

Juckes, M., The mass flux across the tropopause: quasi-geostrophic theory, *Q.J.R. Meteorol. Soc.*, *123*, 71-99, 1997.

Keeling, C.D., J.F.S. Chin, and T.P. Whorf, Increased activity of northern vegetation inferred from atmospheric CO_2 measurements, *Nature*, *382*, 146-149, 1996.

Langford, A.O., C.D. Masters, M.H. Proffitt, E.-Y. Hsie, and A.F. Tuck, Ozone measurements in a tropopause fold associated with a cut-off low system, *Geophys. Res. Lett.*, *23*, 2501-2504, 1996.

Lelieveld, J., B. Bregman, F. Arnold, V. Bürger, P.J. Crutzen, H. Fischer, A. Waibel, P. Siegmund, P.F.J. van Velthoven, Chemical pertubation of the lowermost stratosphere through exchange with the troposphere, *Geophys. Res. Lett.*, *24*, 603-606, 1997.

Levin, I., and V. Hesshaimer, Refining of atmospheric transport model entries by the globally observed passive tracer distribution of ^{85}Kr and sulfur hexafluoride, *J. Geophys. Res.*, *101*, 16,745-16,755, 1996.

Maiss, M., P. Steele, R.J. Francey, P.J. Fraser, R.L. Langenfelds, N.B.A. Trivett, and I. Levin, Sulfur hexafluoride: A powerful new atmospheric tracer, *Atmos. Environ.*, *30*, 1621-1639, 1996.

Marenco, A., M. Macaigne, and S. Prieur, Meridional and vertical CO and CH_4 distributions in the backgrpund troposphere (70°N, 60°S, 0-12 km altitude) from scientific aircraft measurements during the STRATOZ III experiment (June 1984), *Atmos. Environ.*, *23*, 185-200, 1989.

Matsueda, H., H.Y. Inoue, and M. Ishii, Latitudinal distributions of methane in the upper troposphere and marine boundary layer over the Pacific in 1990, *Geophys. Res. Lett.*, *20*, 695-698, 1993.

Mauzerall, D.L., D.J. Jacob, S.-M. Fan, J.D. Bradshaw, G.L. Gregory, G.W. Sachse, and D.R. Blake, Origin of tropospheric ozone at remote high northern latitudes in summer, *J. Geophys. Res.*, *101*, 4175-4188, 1996.

Mote, P.W., J.R. Holton, and B.A. Boville, Characteristics of stratosphere-troposphere exchange in a general circulation model, *J. Geophys. Res.*, *99*, 16,815-16,829, 1994.

Nakazawa, T., K. Miyashita, S. Aoki, and M. Tanaka, Temporal and spatial variations of upper tropospheric and lower stratospheric carbon dioxide, *Tellus*, *43*, *Ser. B*, 106-117, 1991.

Nakazawa, T., S. Morimoto, S. Aoki, and M. Tanaka, Time and space variations of the carbon isotopic ratio of tropospheric carbon dioxide over Japan, *Tellus*, *45*, *Ser. B*, 258-274, 1993.

Nakazawa, T., T. Machida, S. Sugawara, S. Murayama, S. Morimoto, G. Hashida, H. Honda, and T. Itoh, Measurements of the stratospheric carbon dioxide concentration over Japan using a balloon-borne cryogenic sampler, *Geophys. Res. Lett.*, *22*, 1229-1232, 1995.

Nakazawa, T., S. Morimoto, S. Aoki, and M. Tanaka, Temporal and spatial variations of the carbon dioxide ratio of atmospheric carbon dioxide in the western Pacific region, *J. Geophys. Res.*, *102*, 1271-1285, 1997a.

Nakazawa, T., S. Sugawara, G. Inoue, T. Machida, S. Maks-

hyutov, and H. Mukai, Aircraft measurements of the concentrations of CO_2, CH_4, N_2O, and CO and the carbon and oxygen isotopic ratios of CO_2 in the troposphere over Russia, *J. Geophys. Res.*, *102*, 3843-3859, 1997b.

Newman, P.A. and M.R. Schoeberl, A reinterpretation of the data from the NASA stratosphere-troposphere exchange project, *Geophys. Res. Lett.*, *22*, 2501-2504, 1995.

Oltmans, S.J., Climatology of Arctic and Antarctic tropospheric ozone, in *NATO ASI Ser.*, vol. 17, Springer, 25-40, 1993.

Parrish, D.D., M. Trainer, J.S. Holloway, J.E. Yee, M.S. Warshawsky, F.C. Fehsenfeld, G.L. Forbes, and J.L. Moody, Relationships between ozone and carbon monoxide at surface sites in the North Atlantic region, *J. Geophys. Res.*, *103*, 13,357-13,376, 1998.

Patra, P.K., S. Lal, B.H. Subbaraya, C.H. Jackman, and P. Rajaratnam, Observed vertical profiles of sulfur hexafluoride (SF_6) and its atmospheric applications, *J. Geophys. Res.*, *102*, 8855-8859, 1997.

Pollock, W., L.E. Heidt, R.A. Lueb, J.F. Vedder, M.J. Mills, and S. Solomon, On the age of stratospheric air and ozone depletion potentials in the polar regions, *J. Geophys. Res.*, *97*, 12,993-12,999, 1992.

Reed, R.J., A study of a characteristic type of upper level frontogenesis, *J. Meteorol.*, *12*, 226-237, 1955.

Rosenlof, K.H., Seasonal cycle of the residual mean meridional circulation in the stratosphere, *J. Geophys. Res.*, *100*, 5173-5191, 1995.

Rosenlof, K.H., A.F. Tuck, K.K. Kelly, J.M. Russell III, and M.P. McCormick, Hemispheric asymetries in water vapor and inferences about transport in the lower stratosphere, *J. Geophys. Res.*, *102*, 12,213-13,234, 1997.

Schmidt, U., and A. Khedim, In-situ measurements of carbon dioxide in the winter arctic and at midlatitudes: an indicator of the age of stratospheric air, *Geophys. Res. Lett.*, *18*, 763-766, 1991.

Schmidt, M., R. Borchers, P. Fabian, G. Flentje, W.A. Matthews, A. Sabo, and S. Lal, Trace gas measurements during aircraft flights in the tropopause region over Europe and North Africa, *J. Atmos. Chem.*, *2*, 133-143, 1984.

Shapiro, M.A., T. Hampel, and A.J. Krueger, The arctic tropopause fold, *Mon. Weather Rev.*, *115*, 444-454, 1987.

Siegmund, P.C., P.F.J. van Velthoven, and H. Kelder, Cross-tropopause transport in the extratropical northern winter hemisphere, diagnosed from high-resolution ECMWF data, *Q.J.R. Meteorol. Soc.*, *122*, 1921-1941, 1996.

Solomon, S., S. Borrmann, R.R. Garcia, R. Portman, L. Thomason, L.R. Poole, D. Winker, and M.P. McCormick, Heterogenous chlorine chemistry in the tropopause region, *J. Geophys. Res.*, *107*, 21,411-21,429, 1997.

Staley, D.O., Evaluation of potential-vorticity changes near the tropopause and the related vertical motions, vertical advection of vorticity, and transfer of radioactive debris from stratosphere to troposphere, *J. Meteorol.*, *17*, 591-620, 1960.

Strahan, S.E., A.R. Douglass, J.E. Nielsen, and K.A. Boering, The CO_2 seasonal cycle as a tracer of transport, *J. Geophys. Res.*, *103*, 13,729-13,741, 1998.

Tanaka, M., T. Nakazawa, and S. Aoki, Time and space variations of tropospheric carbon dioxide over Japan, *Tellus*, *39, Ser. B*, 3-12, 1987.

Thuburn, J., and G.C. Craig, GCM tests of theories for the height of the tropopause, *J. Atmos. Sci.*, *54*, 869-882, 1997.

Trolier, M., J.W.C. White, P.P. Tans, K.A. Maserie, and P.A. Gemery, Monitoring the isotopic composition of atmospheric CO_2: Measurements from the NOAA Global Air Sampling Network, *J. Geophys. Res.*, *101*, 25,897-25,916, 1996.

VanHaver, P., D. DeMuer, M. Beekmann, and C. Mancier, Climatology of tropopause folds at midlatitudes, *Geophys. Res. Lett.*, *23*, 1033-1036, 1996.

Van Velthoven, P.F.J., and H. Kelder, Estimates of stratosphere-troposphere exchange: sensitivity to model formulation and horizonatal resolution, *J. Geophys. Res.*, *101*, 1429-1434, 1996.

Waugh, D.W., et al., Mixing of polar air into middle latitudes as revealed by tracer-tracer scatterplots, *J. Geophys. Res.*, *102*, 13,119-13,134, 1997.

Woodbridge, E.L., et al., Estimates of total organic and inorganic chlorine in the lower stratosphere from in situ and flask measurements during AASE II, *J. Geophys. Res.*, *100*, 3057-3064, 1995.

Yang, H., and K.K. Tung, Cross-isentropic stratosphere-troposphere exchange of mass and water vapor, *J. Geophys. Res.*, *101*, 9413-9423, 1996.

Zahn, A., V. Barth, K. Pfeilsticker, and U. Platt, Deuterium, Oxygen-18, and Tritium as tracers for water vapour transport in the lower stratosphere and tropopause region, *J. Atmos. Chem.*, *30*, 25-47, 1998a.

Zahn, A., V. Barth, K. Pfeilsticker, and U. Platt, Airborne high-resolution ozone and potential vorticity to study stratospheric-tropospheric exchange, in: Proceedings of the XVIII Quadrennial Ozone Symposium, L'Aquila (Italien), 12-21 Sept. 1996, 1998b.

M. Maiss and A. Zahn, Atmospheric Division, Max-Planck Institute for Chemistry, P.O. Box 3060, D-55020 Mainz, Germany. (e-mail: zahn@mpch-mainz.mpg.de)

R. Neubert, Centrum voor Isotopenonderzoek, University of Groningen, Nijenborgh 4, NL-9747 AG Groningen, Netherlands.

U. Platt, Institute für Umweltphysik, University of Heidelberg, D-69120 Heidelberg, Germany.

(Received June 18, 1998; revised December 8, 1998; accepted December 14, 1998.)